Synergistic developmental regulators enable efficient plant regeneration and transformation across species

Heqiang Huo

hhuo@ufl.edu

University of Florida https://orcid.org/0000-0001-8850-3558

Tao Jiang

University of Florida - IFAS

Zhaoyuan Lian

Northwest A&F University

Keila Rodriguez

University of Florida - IFAS

Fangchen Liu

University of Florida - IFAS

Anandi Karn

University of Florida - IFAS https://orcid.org/0009-0002-9345-0635

Wisnu Handoyo

University of Florida - IFAS

Mohammed Kyum

University of Florida - IFAS

Sameena Ejaz Tanwir

University of Florida - IFAS

Allen Van Deynze

University of California, Davis https://orcid.org/0000-0002-2093-0577

Kent Bradford

University of California, Davis https://orcid.org/0000-0002-9521-6124

Kevin Kenworthy

University of Florida

Patricio Muñoz

University of Florida https://orcid.org/0000-0001-8973-9351

Carlos Messina

University of Florida

Songhu Wang

School of Horticulture, Anhui Agricultural University https://orcid.org/0000-0002-7822-769X

Article

Keywords:

Posted Date: February 3rd, 2026

DOI: https://doi.org/10.21203/rs.3.rs-8622129/v1

Additional Declarations: There is **NO** Competing Interest.

Synergistic developmental regulators enable efficient plant regeneration and transformation across species

Tao Jiang[1,2,3], Zhaoyuan Lian[4], Keila Rodriguez[1,3], Fangchen Liu[1], Anadi Karn[2], Wisnu Handoyo[3], Mohammed Kyum[5], Sameena Ejaz Tanwir[1,3], Allen Van Deynze[6], Kent J. Bradford[6], Kevin Kenworthy[5], Patricio Munoz[3], Carlos D. Messina[1,2], Songhu Wang[7], Heqiang Huo[1,2,3*]

Affiliations

[1] Crop Transformation Center, University of Florida, Gainesville, FL, 32611, U.S.A

Tao Jiang, Keila Rodriguez, Fangchen Liu, Sameena Ejaz Tanwir, Carlos D. Messina, Heqiang Huo

[2] Department of Horticultural Sciences, University of Florida, Gainesville, FL, 32611, U.S.A

Tao Jiang, Keila Rodriguez, Fangchen Liu, Anadi Karn, Wisnu Handoyo, Carlos D. Messina, Heqiang Huo

[3] Mid-Florida Research & Education Center, University of Florida, Apopka, FL, 32703, U.S.A

Tao Jiang, Keila Rodriguez, Fangchen Liu, Wisnu Handoyo, Sameena Ejaz Tanwir, Heqiang Huo

[4] College of Horticulture, Northwest A&F University, Yangling, Shaanxi, 712100, China

Zhaoyuan Lian

[5] Department of Agronomy, University of Florida, Gainesville, FL, 32611, U.S.A

Mohammed Kyum, Kevin Kenworthy

[6] Seed Biotechnology Center, Department of Plant Sciences, University of California, Davis, CA, 95616, U.S.A

Allen Van Deynze, Kent J. Bradford

[7] Anhui Province Key Laboratory of Horticultural Crop Quality Biology, School of Horticulture, Anhui Agricultural University, Hefei, 230036, China

Songhu Wang

Contributions

H.H. and T.J. conceived and designed the experiments. T.J. constructed vectors, initiated DRs screening in chili, performed RNA-seq and data analyses, and co-wrote the manuscript with H.H.. Z.L. conducted *in planta* transformation in Gloxinia. K.R. screened DRs in tomato and chili, and tested them in lettuce and ornamental eggplant. F.L. screened DRs in petunia. A.K. and P.M. tested DRs in blueberry. W.H. tested DRs in begonia. M.K. tested DRs in turfgrass. S.E.T. performed genotyping. H.H., P.M., K.K., K.J.B., S. W., and A.V.D. revised the manuscript.

Corresponding author

Correspondence to: Heqiang Huo (hhuo@ufl.edu; ORCID ID: 0000-0001-8850-3558)

Abstract

Plant genetic transformation is a powerful tool for crop improvement and functional genomics, yet many economically important species remain recalcitrant to current methodologies. To address this limitation, we screened nine developmental regulatory genes (DRs) and sixteen DR combinations, identifying the combination of *PLETHORA5* (*PLT5*) and *GROWTH-REGULATING FACTOR 4/GRF-INTERACTING FACTOR 1* (*GRF4/GIF1*) (labeled as *PLT5-GRFs* combo) as a potent enhancer of regeneration and transformation efficiency. *PLT5-GRFs* combination was effective across diverse plant species, including petunia (*Petunia hybrida*), tomato (*Solanum lycopersicum*), lettuce (*Lactuca sativa*), ornamental eggplant (*Solanum aethiopicum*), and recalcitrant species such as chili pepper (*Capsicum annuum*), begonia (*Begonia semperflorens*), bahiagrass (*Paspalum notatum* Flügge), and blueberry (*Vaccinium corymbosum*). Moreover, it enhanced *in planta* transformation in Gloxinia (*Sinningia speciosa*). Transcriptional profiling revealed that *PLT5-GRFs* synergistically regulates key pathways in development, hormone signaling, epigenetic modifications, and cell fate reprogramming. Our findings establish *PLT5-GRFs* as a universal tool for plant genetic modification, offering a broadly applicable platform in plant biotechnology with profound implications for basic research, crop improvement, and sustainable agriculture.

Introduction

Plant genetic transformation is the foundation of modern plant biotechnology, enabling the introduction of novel traits unattainable through conventional breeding and facilitating functional genomic studies [1]. The advent of CRISPR/Cas technologies has further highlighted the need for efficient transformation systems, as these tools fundamentally rely on effective delivery of editing reagents into plant cells and the subsequent regeneration of genetically modified plants [2]. Despite decades of methodological advances, including Agrobacterium- and biolistic-mediated transformation methods [3-7], the broad application of plant transformation remains severely limited in recalcitrant plant species [8-10]. This recalcitrance to transformation significantly limits the utility of both conventional transgenics and CRISPR-based

technologies, particularly in crops with poor regeneration capacity [3,11]. The strong species and genotype dependence of existing protocols exacerbates this challenge, necessitating the development of more universally applicable strategies to improve efficiency across diverse plant taxa, including monocots and dicots, as well as herbaceous and woody species [12-15]. Current transformation pipelines are often labor-intensive, time-consuming, and require sterile environments, specialized facilities, and skilled personnel. The turnaround time for generating transgenic plants typically ranges from 4 to 12 months for various crops [16,17], creating substantial barriers to fundamental research and crop improvement through biotechnology approaches.

Overcoming transformation recalcitrance involves understanding the molecular mechanisms that govern plant regeneration, a fundamental process underlying successful transformation. Plant regeneration proceeds through precisely orchestrated phases: wound response and cellular dedifferentiation, acquisition of pluripotency and establishment of the stem cell niche, formation of the shoot promeristem and patterning, and finally, shoot regeneration and growth [18,19]. Each phase requires exquisite spatiotemporal coordination of gene expression networks controlled by developmental regulators (DRs), master transcription factors, and signaling proteins that function as molecular switches directing cell fate transitions [20,21].

Recent advances have identified key DR gene families functioning at distinct regeneration phases. During the wound response and dedifferentiation phase, transcription factors like *WOUND INDUCED DEDIFFERENTIATION 1-4* (*WIND1-4*) integrate stress signals with hormonal pathways to promote callus formation [22], with *WIND1* activating dedifferentiation via the *ENHANCER OF SHOOT REGENERATION 1* (*ESR1*) pathway [23]. Pluripotency acquisition and establishment involve *WUSCHEL-related homeobox* (*WOX*) genes (*WOX5*, *WOX11/12/13*) [24,25], *LATERAL ORGAN BOUNDARIES DOMAIN factors* (LBD16/29) [26], and *PLETHORA* family members (*PLT1/2* and *PLT3/5/7*) [27], which collectively maintain auxin gradients and stem cell competence. Subsequent shoot meristem formation and patterning phase requires coordinated action of *CUP-SHAPED COTYLEDON* (*CUC1/2*) [28], *SHOOT*

MERISTEMLESS (*STM*) [29], *ESR1/2*, and *PLT3/5/7* to establish meristem patterning and organ initiation [21]. *WUSCHEL* (*WUS*) activation is pivotal for shoot progenitor formation, fine-tuned by cytokinin signaling through *CLAVATA 3* (*CLV3*) [30]. In the final phase, the *WUS-CLV3-STM* regulatory module maintains shoot apical meristem (SAM) organization, ensuring sustained stem cell division and proper meristem size [31]. Additional major transcription factor families, such as *APETALA2/ETHYLENE RESPONSE FACTOR* (*AP2/ERF*) family and *GROWTH-REGULATING FACTOR* (*GRF*) family [32], as well as genes involved in hormone biosynthesis (e.g., *YUCCA* (*YUC*) [33], *ISOPENTENYLTRANSFERASE* (*IPT*) [34], and *LONELY GUY* (*LOG*) [35], also contribute significantly across multiple regeneration phases.

Ectopic expression of individual DRs has demonstrated remarkable potential for enhancing regeneration and transformation in several plant species. For example, overexpressing *WUS* induces somatic embryogenesis and shoot regeneration in Arabidopsis, tobacco, soybean, cotton, and maize [11,36], while overexpression of other *WOX* family members, such as *WOX5* and *WOX13*, promotes root stem cell identity, adventitious rooting, and shoot regeneration [24,25]. Within the *AP2/ERF* family, *ESR1* enhances shoot regeneration, while *WIND1* is critical for dedifferentiation and callus induction [23]. Similarly, overexpression of *PLT3/5/7* enhances shoot competence and regeneration [27]. The *GRF4/GIF1* (labelled as *GRFs*) chimeric proteins markedly accelerate and improve regeneration in diverse crops such as wheat, triticale, rice, tomato, watermelon, strawberry, and more [12,37-39]. Likewise, overexpression of auxin and cytokinin biosynthesis genes, such as *YUC*, *IPT*, and *LOG*, boosts hormone production, resulting in improved callus formation, shoot regeneration, and embryogenesis [33-35].

Despite significant progress from applying single DRs, successful plant regeneration requires coordinated transitions regulated by multiple transcription factors, hormones, and epigenetic modifications [40]. This suggests that single DRs may not achieve robust and consistent regeneration across different species or genotypes within the species. While the *WUS2-BBM* combination has been studied for the synergistic enhancement of transformation in maize and sorghum [41], its application in dicots has yielded inconsistent results, frequently causing abnormal development or poor regeneration [42]. This highlights the critical need

for systematic evaluation of DR combinations to identify broadly applicable strategies that can reliably enhance transformation frequency across diverse plant species.

Here, we present a comprehensive screening of nine key developmental regulators (*PLT5*, *IPT*, *GRF4/GIF1*, *WUS*, *WIND1*, *ESR1*, *BBM*, *WOX5*, *WOX13*) and sixteen strategic combinations selected based on their established roles across different regeneration phases. Through systematic evaluation across multiple plant species, we identify optimal DR pairings that significantly enhance both regeneration capacity and transformation efficiency. These findings establish broadly applicable strategies to overcome transformation recalcitrance, thereby expanding access to plant biotechnology tools for crop improvement and fundamental research.

Results

Comprehensive evaluation of DRs reveals *PLT5-GRFs* combo enhances regeneration and transformation in petunia and tomato

To systematically assess the effects of developmental regulators (DRs) on plant regeneration and transformation, we evaluated nine single DRs and 16 different DR combinations in petunia and tomato (Fig.1, and Supplementary Figs. 4 and 5).

Individual DRs exhibit limited improvement compared to controls. In petunia, callus induction efficiency varied minimally among most individual DRs, with *PLT5, WIND1*, and *BBM* showing moderate improvement in callus induction, shoot regeneration and transformation compared to the pOX135 control (CK) at 2 and 3 weeks post-inoculation (wpi) (Fig. 1a, b, Supplementary Fig.4, and Supplementary Table 1), whereas *GRF4/GIF1 (*labeled as *GRFs)*, *ESR1*, *WOX5*, *WOX13* had only mild effects impact comparable to the control. (Supplementary Table 1 and Supplementary Fig. 4). Similarly, in tomato, individual DRs showed modest improvements in transformation frequency at 4 wpi, *PLT5* reached 12.29% and *ESR1* achieved 19.83%, yet all remained substantially below the performance of DR combinations except ESR1 (Fig. 1c, d; Supplementary Fig.5, and Supplementary Table 2).

***PLT5-GRFs* combo demonstrates superior performance across species.** Among all DR combinations tested, the combination of *PLT5* and *GRFs* (*PLT5-GRFs*) exhibited the strongest and most consistent improvements across metrics in both species. In petunia, *PLT5-GRFs* significantly improved callus induction efficiency to 72.7% ($P < 0.05$) at 2 wpi and 84.44% ($P < 0.01$) at 3 wpi, representing 29.8% and 20.9% increases over controls, respectively (Fig.1a, b, and Supplementary Table 1). Shoot regeneration was significantly improved using *PLT5-GRFs,* achieving a 5.4-fold increase at 2 wpi (25.08% vs. 4.6% in CK) and a 3.3-fold increase at 3 wpi (53.33% vs. 16.35 % in CK) (Supplementary Table 1). Remarkably, transformation frequency increased 8.9-fold at 2 wpi (41.11% vs. 4.6%) and 3.4-fold at 3 wpi (80.44% vs. 23.71%) (Supplementary Table 1; Supplementary Fig. 4).

In tomatoes, *PLT5-GRFs* demonstrated superior efficacy across all time points. At 3 wpi, callus induction efficiency increased 2.6-fold at 3 wpi (68.89% vs. 26.56% in CK) and remained consistently higher through 5 wpi (73.49% vs. 45.31%) (Supplementary Table 2). Explants transformed with *PLT5-GRFs* showed the earliest and most robust shoot primordia development at 3 wpi (Fig. 1c). This resulted in progressive increases in shoot regeneration efficiency: 13.27% at 3 wpi, 23.57% at 4 wpi, and 37.96% at 5 wpi, compared to 0%, 4.69%, and 7.81% in controls, respectively (Fig. 1c, d; Supplementary Table 2).

Similar to petunia, the most substantial improvement was observed in tomato transformation frequency. By 5 wpi, *PLT5-GRFs* achieved transformation frequencies of 38.86% and 64.21%, representing 8.3- and 5.9-fold increases over controls, respectively, and significantly outperforming all other DR treatments ($P < 0.01$) (Fig. 1b, Supplementary Table 2).

Several other two-gene combinations demonstrated significant improvements over the control but remained inferior to PLT5-GRFs. In tomato at 5 wpi, *PLT5-IPT* achieved 34.83%, *PLT5-WUS* reached 29.58%, and *PLT5-ESR1* attained 42.31% transformation frequency, all significantly improved relative to the controls ($P < 0.05$ or $P < 0.01$), but still substantially lower than *PLT5-GRFs* (64.21%) (Supplementary Fig. 5; Supplementary Table 2).

Adding a third regulator (e.g. *WUS*, *IPT*, *ESR1*, *WOX5*, or *WOX13*) to *PLT5-GRFs* did not yield additive improvements in either species. Triple DR combinations showed callus induction, shoot regeneration, and transformation similar to, or even lower than the *PLT5-GRFs* combination across all timepoints (Supplementary Tables 1 and 2; Fig. 1b, d; Supplementary Fig. 4 and 5). For example, in tomato, *PLT5-GRFs-WOX13* achieved only 22.44% at 5 wpi, substantially lower than *PLT5-GRFs* (64.21%) (Fig. 1b; Supplementary Table 2). The quantitative findings are further supported by visual phenotypes, which showed earlier primordium formation, greater shoot density, and enhanced explant greening on PLT5-GRFs culture plates compared to all other treatments across time points (Supplementary Fig. 5).

PLT5-GRFs combo enhances regeneration and transformation in recalcitrant chili pepper

The efficacy of *PLT5-GRFs* was then evaluated for overcoming the recalcitrance of chili pepper (*Capsicum annuum*), which is a well-documented problem [43,44](Fig. 2; Supplementary Fig. 6; Supplementary Table 3). Among all evaluated DRs, *PLT5-GRFs* exhibited the highest regeneration and transformation performance across timepoints. At 3 wpi, shoot induction efficiency achieved 19.46% shoot induction efficiency and 21.52% transformation frequency, both significantly higher than the control (0% for both metrics) (Supplementary Fig. 6; Supplementary Table 3). By 4 wpi, these improvements became more pronounced, with shoot induction efficiency reaching 36.49% and transformation frequency rising to 56.09%, substantially exceeding those of all other treatments (Fig. 2c-e, Supplementary Table 3). Visual assessment aligned with the quantitative assessments. At 10 days post-inoculation (dpi), *PLT5-GRFs* explants developed robust calli with early shoot primordia formation, while control explants only exhibited minimal callus development (Fig. 2a, b). By 30 dpi, regenerated shoots from *PLT5-GRFs* displayed strong fluorescent signal, supported by strong transgene expression during organogenesis in *PLT5-GRFs* explants at 3 wpi (Fig. 2f) and confirmed with PCR genotyping (Fig. 2h), indicating successful transformation, whereas CK explants remained largely unregenerated. At 60

196 dpi, *PLT5-GRFs* produced well-developed, healthy shoots, while CK explants showed minimal shoot
197 development (Fig. 2c, d). In line with these, more than one third (36.49%) of *PLT5-GRFs* explants
198 developed visible shoot primordia with strong GFP fluorescent signals at 4 wpi (Fig. 2e, Supplementary
199 Fig. 6, Supplementary Fig. 7a),

200 Comparative analysis across all treatments revealed that several other DR combinations demonstrated
201 modest improvements but remained substantially inferior to *PLT5-GRFs* (Supplementary Fig. 6;
202 Supplementary Table 3). Individual explant images showed that while some treatments, like *PLT5-IPT*
203 and *PLT5-GRFs-WOX13*, induced callus formation, their regeneration capacity was markedly lower than
204 that of *PLT5-GRFs*. At 2-, 3-, and 4- wpi, *PLT5-GRFs* explants consistently exhibited the largest, most
205 robust calli with visible shoot primordia. At the same time, other treatments showed smaller, less
206 organized callus structures or minimal regeneration (Supplementary Fig. 6). Quantitatively, the triple
207 combination *PLT5-GRFs-WOX13* achieved 23.17% shoot induction and 31.04 % transformation
208 frequency at 4 wpi (Supplementary Table 3). In comparison, *PLT5-IPT* reached 13.46% shoot
209 regeneration and 28.85% transformation frequency. In contrast, other *PLT5*-based combinations,
210 including *PLT5-WIND1*, *PLT5-WUS*, *PLT5-ESR1*, *PLT5-WOX5*, *PLT5-WOX13*, and *PLT5-BBM,* were
211 significantly less effective, with transformation efficiencies ranging from 7.85% to11.54% at 4 wpi.
212 Individual DRs (*PLT5, GRFs, IPT)* yielded only marginal activity, with transformation efficiencies below
213 6%, while the control explants were almost entirely recalcitrant (1.92 %) (Supplementary Table 3).

214 Phenotypic analysis of *PLT5-GRFs* transgenic chili plants further demonstrated the impact of this
215 treatment combination (Supplementary Fig. 7). In the T_0 generation, transformed plants displayed
216 enhanced visible vegetative vigor, including larger leaves, flowers, and seeds, as well as increased seed
217 size compared with wild-type controls (Supplementary Fig. 7b–d). These traits were stably transmitted to
218 the T_1 generation, which maintained robust growth and normal fertility (Supplementary Fig. 7d).
219 Transgene presence and inheritance were validated by strong GFP fluorescence in multiple tissues,
220 particularly in seeds, and by PCR genotyping in T_1 plants (Fig. 2h; Supplementary Fig. 7c). Quantitative

measurements confirmed a significant increase in plant height in PLT5-GRFs lines (Supplementary Fig. 7e).

Overall, these results establish *PLT5-GRFs* as the most effective regulator module for chili pepper, achieving transformation efficiencies of over 50% (vs. <1.92% for CK; Supplementary Table 3), successfully overcoming the recalcitrance barrier, and enabling the production of stable and fertile transgenic lines, and offering a powerful tool for both functional genomics and crop improvement in chili.

Transcriptional profiling reveals the synergistic effect of *PLT5* and *GRFs* on plant regeneration and transformation

To elucidate the molecular basis for the enhanced regeneration capacity conferred by co-overexpression of *PLT5* and *GRFs* (*PLT5-GRFs)*, we performed RNA sequencing on chili pepper explants at 1- and 3-wpi transformed with either an empty vector control (CK) *PLT5* alone (P), *GRFs* alone (G), or the combination *PLT5-GRFs* (PG) expression constructs (Fig. 3a; Supplementary Fig. 8).

Time-course differential expression analysis revealed distinct patterns across treatments, with PG explants undergoing the most extensive transcriptional reprogramming (Fig. 3b). At 1 wpi, PG treatment resulted in 2,847 upregulated and 1,653 downregulated genes, substantially more than CK, P, or G treatments alone (Fig. 3b, Supplementary Fig. 8). Among the top 10 most significantly regulated genes, PG treatment consistently induced the highest fold-changes in key regeneration-associated factors (Fig. 3c). On the other hand, individual treatments showed more modest effects: P treatment alone activated fewer developmental genes compared to PG, while G treatment showed intermediate responses. Notably, the combination effect was non-additive, suggesting synergistic rather than cumulative gene regulation (Fig. 3, Supplementary Fig. 8).

Kyoto Encyclopedia of Genes and Genomes (KEGG) pathway enrichment analysis showed that DEGs in PG were significantly enriched in pathways critical for regeneration, including plant hormone signal transduction, DNA replication, cell cycle regulation, and chromatin organization (Fig. 3d) Cross-species

validation using homolog analyses in Arabidopsis, tobacco, and tomato confirmed the conservation of these enriched pathways, reinforcing the broad applicability of our findings (Supplementary Fig. 8a–c).

Hierarchical clustering and heatmap analyses revealed distinct expression patterns across treatments (CK, P, G, PG) and time points for key regulatory modules (Fig. 3e-j; Supplementary Fig. 8d-l). Treatment comparison showed that PG induced the most pronounced and sustained upregulation of developmental regulators essential for meristem establishment and shoot regeneration, including *WOX5*, *SHOOT MERISTEMLESS* (*STM*), and *CUP-SHAPED COTYLEDON 1* (*CUC1*), with expression levels significantly higher than did P or G alone (Fig. 3e; Supplementary Fig. 8d). CK treatment showed minimal activation of these genes, while P treatment showed moderate induction and G treatment showed weak responses.

Hormone pathway analysis revealed differential responses among treatments (Fig. 3f, g; Supplementary Fig. 8e, f). PG treatment triggered comprehensive activation of both auxin and cytokinin signaling networks, with cytokinin biosynthesis (*IPT*) and response genes (*ARABIDOPSIS RESPONSE REGULATORS, ARRs*) showing markedly higher expression in PG compared to individual treatments (Fig. 3f, g, Supplementary Fig. 8e, f). Similarly, auxin biosynthesis (*YUCCA*) and transport genes (*PIN, AUX1*) were most strongly activated in *PG*, moderately in *P*, weakly in *G*, and minimally in CK treatments. This hierarchical response pattern (PG > P > G > CK) was consistent across multiple hormone-related pathways (Fig. 3e–f; Supplementary Fig. 8e-f).

Comparative analysis of epigenetic regulatory pathways revealed treatment-specific activation patterns (Fig. 3h–j; Supplementary Fig. 8g–l). *PG* treatment uniquely induced strong upregulation of chromatin remodeling genes, including *SWITCH 3* (*SWI3*) and *FASCIATA 1* (*FAS1*), with expression levels substantially higher than CK and elevated compared to P or G alone (Fig. 3h; Supplementary Fig. 8h). Histone modification enzymes showed similar patterns: *HISTONE DEACETYLASE 6* (*HDA6*)) and histone modifications (*SET DOMAIN GROUP 8* (*SDG8*), *HISTONE METHYLTRANSFERASE 1* (*HMT1*) were most strongly activated in PG, moderately in P, and weakly in G treatments (Fig. 3h-j;

Supplementary Fig. 8g–l). Small RNA processing and DNA modification pathways also showed the strongest activation in PG treatment (Fig. 3i, j; Supplementary Fig. 8i-l). Genes involved in Polycomb Repressive Complex (PRC) interactions and small RNA silencing exhibited the hierarchy PG > P ≥ G > CK, suggesting that the combination treatment creates optimal conditions for comprehensive epigenetic reprogramming necessary for cell fate transitions.

The transcriptional profiling data demonstrate that *PLT5* and *GRFs* function synergistically rather than additively. While individual treatments (P or G) produced modest transcriptional changes, their combination (PG) triggered robust activation of developmental, hormonal, and epigenetic regulatory networks, providing a molecular basis for the superior regeneration efficiency observed with *PLT5-GRFs* treatment.

PLT5-GRFs demonstrates broad-spectrum effectiveness across plant species

To evaluate the versatility of *PLT5-GRFs*, we tested its efficacy in multiple plant species representing different taxonomic groups, including *Begonia semperflorens*, ornamental eggplant (*Solanum aethiopicum*), lettuce (*Lactuca sativa*), blueberry (*Vaccinium corymbosum*), and bahiagrass (*Paspalum notatum,* Flügge). These species encompass ornamentals, leafy vegetables, woody plants, and monocots, each presenting unique challenges in genetic transformation.

In begonia, *PLT5-GRFs* in combination with the visible marker *ROSEA1* (an anthocyanin production regulator) (*PG+RO*) significantly enhanced shoot regeneration and transformation frequency compared to *ROSEA1* alone (*RO*). At 20 dpi, *PG+RO* explants exhibited accelerated callus formation with enhanced GFP fluorescence and red anthocyanin pigmentation, while *RO*-only explants showed weak fluorescence and minimal pigmentation (Supplementary Fig. 9a,b). By 40 dpi, the difference became more pronounced, with *PG+RO* explants displaying intense red pigmentation and strong GFP expression compared to RO controls (Supplementary Fig. 9a,b). At 50 dpi, PG+RO treatment produced significantly more shoots with stronger red coloration and enhanced callus development, whereas RO-only explants

showed limited shoot formation with weak pigmentation (Fig. 4a-d). The enhanced regeneration capacity was clearly evident in culture plates, where PG+RO explants showed substantially higher shoot numbers and more robust development than RO controls (Fig. 4c,d).

At the whole-plant level by 120 dpi, PG+RO-transformed plants displayed vigorous growth with stable red pigmentation distributed throughout leaves, stems, and roots, accompanied by strong GFP expression in both aerial and root tissues under UV illumination (Fig. 4f; Supplementary Fig. 9d). In contrast, wild-type plants exhibited normal green morphology with no visible pigmentation and complete absence of GFP fluorescence (Fig. 4e; Supplementary Fig. 9c). Extended cultivation to 150 dpi confirmed that PG+RO-transformed plants maintained enhanced anthocyanin production and vigorous growth compared to wild-type plants (Supplementary Fig. 9e,f). Quantitative analysis revealed statistically significant improvements ($P < 0.001$) in both callus induction and transformation frequency, with PG+RO achieving a transformation frequency of over 85% compared to less than 10% for the RO-only controls (Fig. 4g, h). These results demonstrate that PLT5-GRFs not only enhance early-stage regeneration but also support stable transgene expression and normal plant development throughout the life cycle.

Similarly, in ornamental eggplant (*Solanum aethiopicum*), PLT5-GRFs (PG) treatment significantly improved transformation outcomes (Supplementary Fig. 10). *PG*-transformed explants developed larger and more compact calli, with early shoot primordia formation by 14 dpi, contrasting sharply with control (CK) explants showing minimal callus development (Supplementary Fig. 10a,b). By 28 dpi, PG explants exhibited distinct shoot primordia emerging from calli, in contrast to CK explants, which displayed minimal or no shoot formation (Supplementary Fig. 10a,b). By 42 dpi, PG-treated explants exhibited higher shoot regeneration frequency and more developed shoots, compared to CK explants (Supplementary Fig. 10c,d). Transformation frequency in PG explants exceeded 75%, compared with less than 40% in CK at both 2- and 3-wpi (Supplementary Fig. 10g,h), with PCR confirmation of transgene integration (Supplementary Fig. 10i).

In lettuce, *PLT5-GRFs* significantly enhanced regeneration and transformation frequency, as evidenced by accelerated shoot emergence and higher transformation rates compared to the RUBY-only control (RU) (Supplementary Fig. 11). By 21 dpi, *PG+RU* explants exhibited early shoot development from callus with red betalain pigmentation, whereas shoot development was much slower from RU-only explants, and no pigmentation was observed from their callus. By 28 dpi, the disparity between treatments was more pronounced, with *PG+RU* explants displaying significantly larger, healthier shoots with intense red pigmentation and strong GFP expression, while control explants continued to show minimal regeneration of smaller shoots (Supplementary Fig. 11a, b). Complete plantlets with roots developed from callus with distinct red pigmentation by 35 dpi, while RU explants continued to show minimal regeneration with smaller shoots (Supplementary Fig. 11c, d). By 90 and 120 dpi, fully regenerated PG+RU plants exhibited vigorous growth with stable red pigmentation throughout leaves, stems, and flowers, along with strong GFP fluorescence, confirming successful transgene integration and expression (Supplementary Fig. 11e, f). In contrast, RU plants exhibited normal green phenotypes with minimal detectable pigmentation in both vegetative and reproductive tissues (Supplementary Fig. 11e, f). Quantitative analysis confirmed that explants transformed with PLT5-GRFs-RUBY (PG+RU) exhibited a 45.4% higher shoot regeneration frequency and a 53.8% higher transformation frequency compared to the RU control (Supplementary Fig. 11g).

Blueberry is a woody species traditionally recalcitrant to transformation. We observed that PLT5-GRFs markedly overcame blueberry transformation barriers (Fig. 5 and Supplementary Fig. 12). The PG+RO-transformed explants exhibited strong GFP fluorescence and distinctive red anthocyanin pigmentation as early as 28 dpi, neither of which was observed in the pOX135 control (CK) (Supplementary Fig. 12a), and this phenotype intensified throughout development up to 70 dpi (Fig. 5b, d, f, h and Supplementary Fig. 12c-e). In contrast, explants transformed with only ROSEA1 (RO-only) displayed minimal pigmentation and no detectable GFP signal (Fig. 5a, c, e, g). By 56 dpi, PG+RO-transformed tissues demonstrated substantially enhanced shoot regeneration compared with RO controls (Fig. 5c, d).

Quantitative analyses revealed that the transformation frequency was significantly higher ($P < 0.01$) in the PG+RO group (Fig. 5j), nearly doubling from approximately 12.1% to 22.7%, while the regeneration frequency was also significantly increased in the PG+RO treatment (Fig. 5c-d, i and Supplementary Fig. 12f-h). The successful integration of the transgene was confirmed by PCR detection of GFP (450 bp) and ROSEA1 (630bp) in two independent T0 transgenic lines from the PG+RO treatment (Fig. 5k, Supplementary Fig. 12i-j). Genotyping showed that 2 out of 5 regenerated seedlings (40.0%) were transgenic in the RO treatment, and 8 out of 12 (66.7%) were transgenic in the PG+RO treatment, using both methods. These results demonstrate that the PLT5-GRFs combination effectively overcomes transformation recalcitrance, even in woody species, while the ROSEA1 visual marker facilitates the identification of successfully transformed tissues throughout the regeneration process.

The effectiveness of PLT5-GRFs extended to monocots, as demonstrated in bahiagrass (*Paspalum notatum* Flügge) transformation. Young leaf explants transformed with PLT5-GRFs produced larger and more compact calli with strong GFP fluorescence (Fig. 6b,d), while control treatments (CK) yielded smaller, loosely organized calli with weak or no GFP signal (Supplementary Fig. 6a, c). At 42 dpi, PG treatment resulted in significantly more regenerated shoots with enhanced growth and development (Fig. 6e, f). By 60 dpi, PG-derived plantlets displayed more vigorous growth and increased biomass accumulation compared to CK plantlets (Fig. 6g, h). Mature transgenic plants derived from PG treatment displayed striking differences in tiller number and overall plant architecture (Fig. 6i, j). Quantitative analysis revealed a significant increase in transformation frequency, expressed as the number of regenerated shoots per explant (Fig. 6k), with PCR confirmation of GFP transgene integration (Fig. 6l).

PLT5-GRFs enhances *in planta* genetic transformation in Gloxinia

To further demonstrate the versatility of PLT5-GRFs beyond conventional tissue culture-based transformation, we developed an efficient *in planta* transformation method for *Sinningia speciosa* (gloxinia) (Fig. 7). We employed a leaf-based vacuum infiltration approach where mature leaves from established plants were mechanically wounded and immersed in Agrobacterium suspension containing

either RUBY alone (RU) or PLT5-GRFs-RUBY (PG+RU) constructs (Fig. 7a). Following vacuum infiltration, leaves were cultivated with petioles embedded in vermiculite to promote regeneration at wound sites.

At 30 dpi, both RU and PG+RU treatments showed initial callus and shoot formation at wound sites, but PG+RU treatment induced multiple transformation events per leaf, with emerging buds displaying strong red pigmentation (Fig. 7b). By 45 dpi, this trend became more evident, with enhanced shoot development and more intense red coloration in PG+RU treatment compared to RU controls (Fig. 7b). PG+RU-transformed leaves consistently exhibited strong GFP fluorescence under UV illumination, providing a secondary confirmation of transformation success (Fig. 7c). However, chimeric buds with both pink and green sectors were observed, suggesting independent transformation events in the absence of selection pressure (Fig. 7b, c).

Remarkably, the regeneration efficiency was significantly higher ($P < 0.05$) in PG+RU treatments than in RU controls, with a nearly 1.5-fold increase (Fig. 7d, left). More strikingly, the transformation frequency increased by approximately 4-fold in PG+RU treatments ($P < 0.01$), rising from ~5% to ~20% (Fig. 7d, right). The stable integration of transgenes in regenerated shoots was confirmed by PCR detection of the GFP gene (450 bp) in multiple independent T0 transformants (Fig. 7e).

This streamlined *in planta* transformation approach, combining vacuum infiltration with PLT5-GRFs, demonstrates significant potential for enhancing transformation frequency without the labor-intensive requirements of traditional tissue culture methods. The combination of PLT5-GRFs facilitates *de novo* shoot regeneration from mature tissues while enabling visual tracking through compatible marker systems. This approach expands the utility of PLT5-GRFs beyond conventional tissue culture methods, offering a streamlined path for genetic modification in species where traditional transformation methods may be challenging.

Discussion

Plant genetic transformation remains a fundamental bottleneck in functional genomics and crop improvement, with many economically important species exhibiting recalcitrant behavior that limits the application of modern biotechnological tools [45-48]. Despite decades of optimization in tissue culture conditions and Agrobacterium-mediated protocols, transformation methods available today have remained largely unchanged since the 1990s, necessitating innovative approaches to overcome species- and genotype-dependent limitations [49,50]. In this study, we systematically screened nine developmental regulators (DRs) and their combinations to identify the most effective factors for enhancing regeneration and transformation across diverse plant species, with a particular focus on the transformation-resistant chili pepper.

Our systematic screening identified the *PLT5-GRFs* combination as a robust solution for overcoming transformation recalcitrance. It significantly improved callus induction, shoot regeneration, and transformation frequency compared to the control and other tested DRs. The synergistic effect of *PLT5* and *GRF4/GIF1* on regeneration and transformation may be attributed to their complementary roles in cell fate reprogramming and coordinated regulation of key developmental processes (Fig. 1; Fig. 3, Fig. 8). *PLT5* functions as a master regulator to establish pluripotency and initiate shoot regeneration by upregulating stem cell regulators and interacting with patterning factors [51,52], while *GRF4/GIF1* promotes cell proliferation and growth through the activation of cell cycle genes and expansins [12,53,54] (Fig. 8a, b). Notably, both *PLT5* and *GRF4* are highly conserved across plant species (Fig. 8b), which likely underlies the broad applicability of this combination across diverse genetic backgrounds. This synergistic interaction explains why *PLT5-GRFs* with additional regulators did not provide an additive benefit, as this module already optimally balances the key regulatory networks required for efficient regeneration.

Transcriptomic analysis in chili pepper revealed the molecular mechanisms underlying *PLT5-GRFs* enhanced regeneration. The *PLT5-GRFs* treatment triggers a coordinated multi-network response involving developmental, hormonal, and epigenetic regulatory pathways (Fig. 3e-j, Fig. 8c; Supplementary Fig. 8d-i). The non-additive gene expression patterns observed with the combination

treatment demonstrate true synergy rather than simple cumulative effects. This comprehensive transcriptional reprogramming involves three key mechanisms (Fig. 8). 1) Developmental Network Activation: *PLT5-GRFs* upregulated critical meristem regulators, including *WOX5, STM*, and *CUC1*, establishing the transcriptional framework necessary for shoot regeneration. This finding corroborates recent evidence that developmental regulators can overcome transformation recalcitrance by promoting cellular differentiation in species previously considered intractable [11,25]. 2) Hormonal Pathway Coordination: The combination treatment simultaneously activated both auxin and cytokinin signaling networks, creating an optimal hormonal environment for cell fate transitions [19,55]. The hierarchical response pattern (PG > P > G > CK) observed across hormone-related genes suggests that *PLT5-GRFs* integration optimizes endogenous hormone production and responsiveness. 3) Epigenetic Reprogramming: Unique to *PLT5-GRFs* treatment was the coordinated activation of chromatin remodeling complexes and histone-modifying enzymes. This epigenetic reprogramming likely facilitates stable cell-fate transitions necessary for sustained regeneration competence, addressing what recent reviews identify as a key factor underlying recalcitrance in plant biotechnology [18,56-58].

The consistent effectiveness across phylogenetically diverse species demonstrates the broad taxonomic applicability of *PLT5-GRFs*. The consistent efficacy of *PLT5-GRFs* across phylogenetically diverse species, from herbaceous crops (lettuce, tomato) to woody perennials (blueberry) and monocots (bahiagrass), demonstrates the universal nature of this approach. These species represent a wide range of plant families, including *Solanaceae*, *Asteraceae*, *Cucurbitaceae*, *Poaceae*, and *Ericaceae*, each with its own unique challenges in genetic transformation [45,59,60]. The consistent enhancement of regeneration and transformation across such diverse species suggests that the *PLT5-GRFs* module targets conserved pathways and mechanisms that are fundamental to plant regeneration [19,61].The broad applicability of *PLT5-GRFs* across species can be attributed to the conserved functions of these genes in regulating key developmental processes. *PLT* genes have been shown to play crucial roles in stem cell maintenance, cell fate determination, and organ patterning in diverse plant species, including Arabidopsis, snapdragon, and

tomato [27,62,63]. Similarly, *GRF-GIF* modules have been implicated in the control of cell proliferation, leaf growth, and regeneration in a wide range of species, such as Arabidopsis, rice, maize, and tomato [64-67]. The evolutionary conservation of these key regulators across diverse plant lineages supports their potential as universal tools for enhancing regeneration and transformation [19].

The success of *PLT5-GRFs* in both in vitro and in planta transformation systems represents a crucial advancement for practical applications. While *in vitro* regeneration remains the primary method for plant transformation [45], *in planta* approaches offer several advantages, such as reduced time, labor, and cost, and the ability to transform recalcitrant species or those with long juvenile phases [59,68]. The development of efficient *in planta* transformation methods is particularly important for species that are difficult to regenerate or those with complex tissue culture requirements [69,70]. The *in planta* transformation results with *Sinningia speciosa* in this study, showing 4-fold enhancement in transformation frequency, demonstrate that *PLT5-GRFs* can overcome barriers even in mature plant tissues (Fig. 7). This capability is particularly valuable for promoting cellular differentiation without requiring external hormone applications, simplifying protocols, and reducing variability.

The *in planta* transformation approach, when combined with *PLT5-GRFs*, could have significant implications for basic research, crop improvement, and plant biotechnology applications. For example, it could facilitate the functional characterization of genes in non-model species or those with long generation times, as it bypasses the need for time-consuming tissue culture steps [59]. *In planta* transformation could also enable the rapid generation of transgenic plants for studying plant-pathogen interactions, as the modified tissues can be directly challenged with pathogens without the need for regeneration [71] Furthermore, this approach could be particularly valuable for crops with complex genomes or those that are recalcitrant to *in vitro* regeneration, such as many woody species [13,60].

Strategies for segregating *PLT5-GRFs* from transformed and edited plants enable practical deployment across different application scenarios. While the PLT5-GRFs system dramatically enhances transformation frequency, practical deployment in crop improvement requires strategies to

remove or silence DR transgenes from final products, both to avoid developmental consequences of constitutive DR expression and to meet regulatory requirements. For conventional genetic transformation, a co-transformation strategy using separate vectors, one carrying *PLT5-GRFs* with a visual marker (e.g., ROSEA1 or RUBY) and another harboring the desired transgene with an independent selectable marker, could enable the generation of transformants containing only the gene of interest through subsequent segregation [72]. In sexually propagated species, the unlinked T-DNAs segregate independently by Mendelian inheritance, allowing selection of progeny carrying only the trait gene while the DR cassette is eliminated. Visual markers can facilitate rapid identification of DR-free individuals in segregating populations [73,74]. For species where sexual segregation is impractical, such as vegetatively propagated crops or those with long juvenile phases, chemically inducible promoter systems (e.g., dexamethasone- or estradiol-responsive elements) can restrict *PLT5-GRFs* expression exclusively to the transformation and regeneration phases, after which DR activity is silenced during normal plant development [75,76]. This approach would allow the benefits of DR-enhanced transformation while minimizing pleiotropic effects in regenerated plants.

For CRISPR-based genome-editing applications, similar strategies apply, with additional considerations. When *PLT5-GRFs* is combined with CRISPR/Cas components on the same T-DNA, the entire editing machinery, including DRs, Cas nuclease, and guide RNAs, can be co-segregated away from the edited locus in seed-propagated species, yielding transgene-free edited plants that face a more streamlined regulatory pathway than conventional transgenics in many jurisdictions [12]. Alternatively, placing *PLT5-GRFs* and CRISPR components on separate vectors allows independent segregation, providing flexibility to retain the editing machinery for additional modifications while eliminating the DRs. An exciting future direction involves establishing "CRISPR host plants" in recalcitrant species, in which *PLT5-GRFs* and the CRISPR/Cas9 machinery are stably integrated into a base genotype. Guide RNAs targeting different genomic loci could subsequently be delivered via nanoparticle-based methods or localized application to wound sites and meristems [2,77]. This platform would enable iterative genome editing of multiple targets

without repeated transformation cycles, substantially accelerating functional genomics and breeding programs in species with long juvenile phases, vegetative propagation, or complex reproductive biology. For seed-propagated species, edited loci and T-DNA insertions could segregate in subsequent generations to obtain transgene-free edited plants. Combined with the visual marker systems demonstrated in this work, such integrated approaches could facilitate both the identification and segregation of desired editing events, ultimately bridging the gap between laboratory innovation and commercial deployment.

In conclusion, our study establishes PLT5-GRFs as a potent and versatile combination for enhancing regeneration and transformation frequency across diverse plant species, including chili pepper, a transformation-recalcitrant species. Its successful application in both *in vitro* and *in planta* systems, supported by comprehensive screening and transcriptomic analysis, reveals key molecular pathways and gene regulatory networks driving regenerative capacity. This system's broad applicability, compatibility with visual markers, and potential for *in planta* methods position it as a transformative tool for plant biotechnology, enabling functional genomics, genetic improvement of economically important crops, and protocols for other recalcitrant species.

Despite these advances, limitations remain, including untested efficacy in additional high-value recalcitrant species and the need for deeper mechanistic insights into PLT5-GRFs' synergistic effects, interactions with developmental regulators or hormone pathways, and long-term transgenic plant stability across generations and environments. Future research should investigate tissue-specific or inducible promoters to minimize pleiotropic effects and integrate PLT5-GRFs with tools such as CRISPR-Cas for precise genetic manipulation. Ultimately, addressing these areas will fully harness the potential of PLT5-GRFs, overcoming species-specific barriers, accelerating crop improvement, synthetic biology, and metabolic engineering, and unlocking the genetic potential of plants to tackle challenges in agriculture, conservation, and research.

Methods

Plant materials and growth conditions

Nine plant species were used for transformation experiments. For in vitro transformation, petunia (*Petunia × hybrida, Cv* 'Mitchell', tomato (*Solanum lycopersicum cv. 'MicroTom'*), lettuce (*Lactuca sativa, cv. 'Salinas'*), chili pepper (*Capsicum annuum, cv. 'CM334'*), ornamental eggplant (*Solanum aethiopicum, cv.* '*Pumpkin-on-a-Stick'*), begonia (*Begonia semperflorens cv. 'UF183-11'*), blueberry (*Vaccinium corymbosum,* Southern Highbush Blueberry*, cv'Albus'*), and bahiagrass (*Paspalum notatum,* Flügge *cv. 'Pensacola'*) were used; For *in planta* transformation, Gloxinia (*Sinningia speciosa, cv. 'Early Giant'*) was used. Unless otherwise specified, all plants were grown and maintained under standard greenhouse conditions, with a 16-hour light/8-hour dark photoperiod at 25°C.

Vector construction

All constructs were based on the pOX135 binary expression vector, which contains a fused eGFP-NPTII gene under a double-enhanced Cassava Vein Mosaic Virus (dCsVMV) promoter, enabling dual selection via fluorescent tracking and kanamycin resistance [78] (Supplementary Fig. 1a).

Single DR overexpression constructs: The coding regions of developmental regulators from Arabidopsis thaliana, including *PLT5* (AT5G57390), *IPT* (DQ058764.1), *WUS* (AT2G17950), *BBM* (AT5G17430), *WOX5* (AT3G11260), *WOX13* (AT4G35550), *ESR1* (AT1G12980), and *WIND1* (AT1G78080), were synthesized (Gene Universal Inc., USA) or PCR-amplified from Arabidopsis thaliana Columbia ecotype using gene-specific primers with flanking *BsaI* sites designed using Primer3Plus [79] (Table S4). These DR fragments were cloned into pOX135 via its *BsaI* sites (Fig. S1A, Table S4). The grape (*Vitis vinifera*) *GRF4* (LOC100259737) and *GIF1* (LOC100253609) genes were fused based on a previously reported construct with modifications to remove some internal restriction sites (Supplementary information 1), and the resulting chimeric gene was synthesized and cloned into pOX135. Expression of these single DRs was driven by a 2×CaMV35S promoter containing an Omega enhancer from pGWB402 (AB294426.1) (Supplementary Fig. 1a).

Multiple DR overexpression constructs: For double DR combinations, each single DR expression cassette (comprising the 2×CaMV35S promoter, coding region, and HSter terminator) was PCR-amplified from its respective pOX135-single DR vector using primers MluI-35S-F and HSter-AatII-R (Supplementary Table S4). These cassettes were then ligated sequentially into pOX135-single DR vectors at the AatII and MluI restriction sites to form different combinations of double DR overexpression constructs (Supplementary Fig. 1b). For triple DR constructs, additional single DR cassettes were PCR-amplified using primers SpeI-35S-F and HSter-SalI-R (Supplementary Table S4) and ligated into pOX135-double DR vectors at the SpeI and SalI restriction sites (Supplemental Fig. 1c).

Reporter gene constructs and combinations with DRs:

The anthocyanin biosynthesis regulator *ROSEA1* (*RO*) (DQ275529.1), from *Antirrhinum majus* [80], as well as the synthetic betalain biosynthetic gene *RUBY* from *Mirabilis jalapa* [57], were used as visual markers. *ROSEA1* was synthesized in Gene Universal Inc (Newark, DE), while the *RUBY* cassette was PCR-amplified from plasmid 35S:RUBY (AddGene: #160908), and cloned into pOX135 at the BsaI cloning sites to form the pOX135-ROS, pOX135-RUBY (Supplementary Fig. 3a). To create combined DR and reporter constructs, the *PLT5* (2×CaMV35S::PLT5::HSter) and *GRF4/GIF1* (2×CaMV35S::GRF4/GIF1::HSter) cassettes were amplified from their respective pOX135-single DR vectors using MluI/AatII and SpeI/SalI primers, respectively, and ligated to pOX135-ROSEA1 or pOX135-RUBY to form pOX135-ROSEA1 -PLT5-GRFs and pOX135-RUBY-PLT5-GRFs (Supplementary Fig. 3a and b).

All plasmids were validated via digestion (Supplementary Fig. 2a-e) and confirmed by Sanger sequencing. The final constructs were introduced into *Agrobacterium tumefaciens* strain EHA105 or GV3101 using the freeze-thaw method [81].

Plant transformation

In-vitro transformation and DR screening: Agrobacterium-mediated *in vitro* transformation was performed to evaluate the effects of different DRs. All transformation experiments included biological replicates; explant numbers (n) are reported in the corresponding Results and figure legends. *A. tumefaciens* strains EHA105 harboring the indicated binary vectors were first cultured in 5ml LB broth at 28°C and 180 rpm overnight. A secondary culture was initiated by inoculating 1 mL of the overnight culture into 10 mL of fresh LB broth, harvesting at an optical density (OD600) of 0.3–0.5, and resuspending in MS liquid medium containing 100 μM acetosyringone.

Petunia transformation: Cotyledon explants from 7- to 10-day-old petunia seedlings were inoculated and cultured on callus induction medium (CIM: MS salts and vitamins, 1 mg l^{-1} BAP, 0.1 mg l^{-1} NAA, and 100 mg l^{-1} kanamycin, and 100 mg l^{-1} Timentin for 2, 3, or 4 weeks [82].

Tomato transformation: Cotyledon explants from 7- to 10-day-old tomato seedlings were inoculated and cultured on CIM (MS salts and vitamins, 2 mg l^{-1} zeatin, 0.2 mg l^{-1} NAA, 100 mg l^{-1} kanamycin, and 100 mg l^{-1} Timentin) for 2, 3, 4, or 5 weeks [78].

Chili pepper transformation: Cotyledon explants from 10- to 14-day-old chilli pepper seedlings were inoculated and cultured on CIM (MS medium supplemented with 3 mg l^{-1} zeatin, 0.3 mg l^{-1} NAA, 100 mg l^{-1} kanamycin, and 100 mg l^{-1} Timentin) for 2, 3, or 4 weeks, then transferred to shoot induction medium (SIM: MS salts and vitamins, 2 mg l^{-1} zeatin, 0.1 mg l^{-1} NAA, 100 mg l^{-1} kanamycin, and 100 mg l^{-1} Timentin) for an additional four weeks. Root induction was conducted on root induction medium (RIM) containing 1/2 MS salts and vitamins, 1 mg l^{-1} IBA, 50 mg l^{-1} kanamycin, and 100 mg l^{-1} Timentin.

Callus induction efficiency (% of explants forming callus), shoot induction efficiency (% of explants forming shoots), and transformation frequency(% of explants forming GFP-positive shoots) were calculated as previously described [83-85]. The top-performing combination of *PLT5-GRFs* was further tested in lettuce, ornamental eggplant, begonia, bahiagrass, and blueberry using established protocols [78,86-89]. Detailed media formulations and culture conditions for each species are provided in Supplementary Methods.

In planta transformation: A dipping-vacuum method was used to transform mature leaves from 4- to 5-month-old Gloxinia plants. Leaves were scratched, immersed in suspension of *A. tumefaciens* strain GV3101 (O.D.=0.5-0.8 in liquid MS supplemented with 100 µM acetosyringone and 2.0 mg l^{-1} silver nitrate), and vacuum-infiltrated at -40 kPa, for 2 min. After infiltration, leaves were incubated under low-light conditions for 2 weeks before being transferred to natural light. Petioles were inserted into moist vermiculite in the tray with a ventilated plastic dome to maintain moisture for subsequent culture and plant regeneration.

Molecular and phenotypic analysis

GFP detection and PCR genotyping: GFP fluorescence was detected using a Leica DM6000 B fluorescent microscope equipped with a GFP filter set [90]. Genomic DNA was extracted from leaf tissues using the CTAB method [91]. PCR was performed using Q5 Hot Start High-Fidelity DNA polymerase (New England BioLabs, USA) according to the manufacturer's instructions. Primers specific for the eGFP-NPTII gene and for T-DNA backbone regions (Supplementary Table S4) were used to confirm stable transgene integration and exclude transient transformation. Amplified DNA fragments were separated by electrophoresis and stained with SYBR Safe (Thermo Scientific, USA) and visualized with the Omega Lum™ Imaging system (Gel Company, USA).

RNA extraction and RT-qPCR analysis: Total RNA was isolated using RNAzol RT (Molecular Research Center, USA), and cDNA was synthesized from 1 µg of total RNA using the QuantiTect Reverse Transcription Kit (Qiagen, Germany) and diluted 25-fold. RT-qPCR reactions were performed using gene-specific primers (Table S5) on the CFX96 real-time PCR system (Bio-Rad, USA) using Bio-Rad SYBR Green Master Mix. Relative expression levels were calculated using the $2^{-\Delta\Delta Ct}$ method [92] with a species-specific housekeeping gene (Actin and GAPDH) as the reference gene [93] (Table S5).

RNA-Seq and data analysis: Total RNA was extracted from chilli explants at 1-, 2-, and 3-weeks post-transformation with empty vector control (CK), PLT5 (P), GRFs (G), or PLT5-GRFs (PG) constructs

using RNAzol RT(Molecular Research Laboratory, USA). RNA quality and quantity were assessed using a Bioanalyzer 2100 (Agilent Technologies, USA). RNA sequencing libraries were prepared using the TruSeq RNA Sample Preparation Kit v2 (Illumina, USA) and sequenced on an Illumina HiSeq 2500 platform (Illumina, USA). RNA sequencing result will be deposited in NCBI GEO upon acceptance. Raw reads were filtered, and clean reads were mapped to the chili pepper reference genome [94] using HISAT2 [95]. Differentially expressed genes (DEGs) were identified using DESeq2 [96] with a false discovery rate (FDR) < 0.05 and |log2(fold change) | ≥ 1. KEGG pathway enrichment analysis of DEGs was performed using the clusterProfiler package in R [97].

Statistical analysis

All statistical analyses were performed using R software [98]. Data normality was assessed using the Shapiro-Wilk test, and homogeneity of variances using Levene's test [99]. When assumptions of parametric tests were violated, data were transformed or analyzed using non-parametric alternatives [100]. Depending on the experimental design and data structure, comparisons between groups were performed using Student's *t*-test, one-way ANOVA followed by Tukey's HSD post-hoc test, or non-parametric tests, such as the Mann-Whitney U test or the Kruskal-Wallis test [101]. Significant differences were determined at the $p < 0.05$ or 0.01 level. Graphs were generated using the ggplot2 package in R.

Data Availability

The data supporting the findings of this study are available upon reasonable request from the corresponding author.

References

1 Jinek, M. *et al.* A programmable dual-RNA–guided DNA endonuclease in adaptive bacterial immunity. *science* **337**, 816-821 (2012).

2 Demirer, G. S. *et al.* Nanotechnology to advance CRISPR–Cas genetic engineering of plants. *Nature Nanotechnology* **16**, 243-250 (2021).

3 Ozyigit, I. I. & Yucebilgili Kurtoglu, K. Particle bombardment technology and its applications in plants. *Molecular biology reports* **47**, 9831-9847 (2020).

4 Sharma, S., Pawar, S., Sagwal, V. & Mishra, C. Genetic transformation methods in plants-"A Review". *International Journal of Agricultural Science* **8** (2023).

5 Su, W., Xu, M., Radani, Y. & Yang, L. Technological development and application of plant genetic transformation. *International Journal of Molecular Sciences* **24**, 10646 (2023).

6 Wu, M. *et al.* Advancements in delivery strategies and non-tissue culture regeneration systems for plant genetic transformation. *Advanced biotechnology* **2**, 34 (2024).

7 Shivashakarappa, K., Marriboina, S., Dumenyo, K., Taheri, A. & Yadegari, Z. Nanoparticle-mediated gene delivery techniques in plant systems. *Frontiers in Nanotechnology* **7**, 1516180 (2025).

8 Belaffif, M. B., Brown, M. C., Marcial, B., Baysal, C. & Swaminathan, K. New strategies to advance plant transformation. *Current opinion in biotechnology* **91**, 103241 (2025).

9 Luo, G. *et al.* Unlocking in vitro transformation of recalcitrant plants. *Trends in Plant Science* (2025).

10 Youngstrom, C., Wang, K. & Lee, K. Unlocking regeneration potential: harnessing morphogenic regulators and small peptides for enhanced plant engineering. *The Plant Journal* **121**, e17193 (2025).

11 Lowe, K. *et al.* Morphogenic regulators Baby boom and Wuschel improve monocot transformation. *The Plant Cell* **28**, 1998-2015 (2016).

12 Debernardi, J. M. *et al.* A GRF–GIF chimeric protein improves the regeneration efficiency of transgenic plants. *Nature biotechnology* **38**, 1274-1279 (2020).

13 Maharjan, B. K. *et al.* Woody Plant Transformation: Current Status, Challenges, and Future Perspectives. *Plants* **14**, 3420 (2025).

14 Nivya, V. & Shah, J. M. Recalcitrance to transformation, a hindrance for genome editing of legumes. *Frontiers in Genome Editing* **5**, 1247815 (2023).

15 Bennur, P. L., O'Brien, M., Fernando, S. C. & Doblin, M. S. Improving transformation and regeneration efficiency in medicinal plants: insights from other recalcitrant species. *Journal of Experimental Botany* **76**, 52-75 (2025).

16 Kausch, A. P. *et al.* Edit at will: genotype independent plant transformation in the era of advanced genomics and genome editing. *Plant Science* **281**, 186-205 (2019).

17 Xu, D. & Yang, L. Regeneration and defense: unveiling the molecular interplay in plants. *New Phytologist* **246**, 2484-2494 (2025).

18 Lee, K. & Seo, P. J. Dynamic epigenetic changes during plant regeneration. *Trends in plant science* **23**, 235-247 (2018).

19 Ikeuchi, M. *et al.* Molecular mechanisms of plant regeneration. *Annual review of plant biology* **70**, 377-406 (2019).

20 Marhava, P. *et al.* Re-activation of stem cell pathways for pattern restoration in plant wound healing. *Cell* **177**, 957-969. e913 (2019).

21 Shin JinWoo, S. J., Bae SoonHyung, B. S. & Seo PilJoon, S. P. De novo shoot organogenesis during plant regeneration. 63-72 (2020).

22 Iwase, A. *et al.* The AP2/ERF transcription factor WIND1 controls cell dedifferentiation in Arabidopsis. *Current Biology* **21**, 508-514 (2011).

23 Iwase, A. *et al.* WIND1 promotes shoot regeneration through transcriptional activation of ENHANCER OF SHOOT REGENERATION1 in Arabidopsis. *The Plant Cell* **29**, 54-69 (2017).

24 Hu, X. & Xu, L. Transcription factors WOX11/12 directly activate WOX5/7 to promote root primordia initiation and organogenesis. *Plant Physiology* **172**, 2363-2373 (2016).

25 Ikeuchi, M. *et al.* Wound-inducible WUSCHEL-RELATED HOMEOBOX 13 is required for callus growth and organ reconnection. *Plant Physiology* **188**, 425-441 (2022).

26 Xu, C. & Hu, Y. The molecular regulation of cell pluripotency in plants. *Abiotech* **1**, 169-177 (2020).

27 Lian, Z. *et al.* Application of developmental regulators to improve in planta or in vitro transformation in plants. *Plant Biotechnology Journal* **20**, 1622-1635 (2022).

28 Hake, S. Vol. 31 1202-1203 (American Society of Plant Biologists, 2019).

29 Cao, X., Du, Q., Guo, Y., Wang, Y. & Jiao, Y. Condensation of STM is critical for shoot meristem maintenance and salt tolerance in Arabidopsis. *Molecular Plant* **16**, 1445-1459 (2023).

30 Shpak, E. D. & Uzair, M. WUSCHEL: The essential regulator of the Arabidopsis shoot Apical Meristem. *Current Opinion in Plant Biology* **85**, 102739 (2025).

31 Su, Y. H. *et al.* Integration of pluripotency pathways regulates stem cell maintenance in the Arabidopsis shoot meristem. *Proceedings of the National Academy of Sciences* **117**, 22561-22571 (2020).

32 Luo, G. & Palmgren, M. GRF-GIF chimeras boost plant regeneration. *Trends in Plant Science* **26**, 201-204 (2021).

33 Liu, Y. *et al.* Transcriptomic and hormonal analyses reveal that YUC-mediated auxin biogenesis is involved in shoot regeneration from rhizome in Cymbidium. *Frontiers in Plant Science* **8**, 1866 (2017).

34 Kshetry, A. O. *et al.* A synthetic transcription cascade enables direct in planta shoot regeneration for transgenesis and gene editing in multiple plants. *Molecular Plant* (2025).

35 Chen, L., Jameson, G. B., Guo, Y., Song, J. & Jameson, P. E. The LONELY GUY gene family: from mosses to wheat, the key to the formation of active cytokinins in plants. *Plant Biotechnology Journal* **20**, 625-645 (2022).

36 Bakulin, S. D., Monakhos, S. G. & Bruskin, S. A. Morphogenetic Factors as a Tool for Enhancing Plant Regeneration Capacity During In Vitro Transformation. *International Journal of Molecular Sciences* **26**, 8583 (2025).

37 Tang, Y. *et al.* Genotype-dependent enhancement of tomato transformation and regeneration by GRF4 and GIF1. *Plant Growth Regulation* **105**, 1789-1801 (2025).

38 Sanchez, E. R. *et al.* Overexpression of Vitis GRF4-GIF1 improves regeneration efficiency in diploid Fragaria vesca Hawaii 4. *Plant Methods* **20**, 160 (2024).

39 Feng, Q. *et al.* Highly efficient, genotype-independent transformation and gene editing in watermelon (Citrullus lanatus) using a chimeric ClGRF4-GIF1 gene. *Journal of integrative plant biology* **63**, 2038-2042 (2021).

40 Wang, P. *et al.* Plant genetic transformation: achievements, current status and future prospects. *Plant Biotechnology Journal* **23**, 2034-2058 (2025).

41 Wang, N. *et al.* Leaf transformation for efficient random integration and targeted genome modification in maize and sorghum. *Nature plants* **9**, 255-270 (2023).

42 Lee, K. & Wang, K. Strategies for genotype-flexible plant transformation. *Current Opinion in Biotechnology* **79**, 102848 (2023).

43 Tang, Y. *et al.* Establishment of an efficient Agrobacterium-mediated transformation system for chilli pepper and its application in genome editing. *Plant Biotechnology Journal* **23**, 4752 (2025).

44 Kumar, R. V., Sharma, V., Chattopadhyay, B. & Chakraborty, S. An improved plant regeneration and Agrobacterium-mediated transformation of red pepper (Capsicum annuum L.). *Physiology and Molecular Biology of Plants* **18**, 357-364 (2012).

45 Altpeter, F. *et al.* Advancing crop transformation in the era of genome editing. *The Plant Cell* **28**, 1510-1520 (2016).

46 Belhaj, K., Chaparro-Garcia, A., Kamoun, S. & Nekrasov, V. Plant genome editing made easy: targeted mutagenesis in model and crop plants using the CRISPR/Cas system. *Plant methods* **9**, 39 (2013).

47 Kothari, S., Joshi, A., Kachhwaha, S. & Ochoa-Alejo, N. Chilli peppers—a review on tissue culture and transgenesis. *Biotechnology advances* **28**, 35-48 (2010).

48 S. Sanghera, G., H. Wani, S., Hussain, W. & B. Singh, N. Engineering cold stress tolerance in crop plants. *Current genomics* **12**, 30-43 (2011).

49 Aboofazeli, N. *et al.* Conquering Limitations: Exploring the Factors that Drive Successful Agrobacterium-Mediated Genetic Transformation of Recalcitrant Plant Species. *Molecular Biotechnology* **67**, 3010-3026 (2025).

50 Maren, N. A. *et al.* Genotype-independent plant transformation. *Horticulture Research* **9**, uhac047 (2022).

51 Kareem, A. *et al.* PLETHORA genes control regeneration by a two-step mechanism. *Current Biology* **25**, 1017-1030 (2015).

52 Prasad, K. *et al.* Arabidopsis PLETHORA transcription factors control phyllotaxis. *Current Biology* **21**, 1123-1128 (2011).

53 Debernardi, J. M. *et al.* Post-transcriptional control of GRF transcription factors by micro RNA miR396 and GIF co-activator affects leaf size and longevity. *The Plant Journal* **79**, 413-426 (2014).

54 Omidbakhshfard, M. A., Proost, S., Fujikura, U. & Mueller-Roeber, B. Growth-regulating factors (GRFs): a small transcription factor family with important functions in plant biology. *Molecular plant* **8**, 998-1010 (2015).

55 Sanchez-Corrionero, A. *et al.* Fine-tuned nitric oxide and hormone interface in plant root development and regeneration. *Journal of Experimental Botany* **74**, 6104-6118 (2023).

56 Hemenway, E. A. & Gehring, M. Epigenetic regulation during plant development and the capacity for epigenetic memory. *Annual Review of Plant Biology* **74**, 87-109 (2023).

57 He, Y., Xu, L. & Liu, Q. The cellular epigenetic blueprint of plant regeneration. *Current Opinion in Plant Biology* **88**, 102784 (2025).

58 Lian, Z. *et al.* Auxin affects gene editing efficiency through regulating chromatin accessibility and plant regeneration process. *Horticulture Research* **12**, uhaf240 (2025).

59 Keshavareddy, G., Kumar, A. & Ramu, V. S. Methods of plant transformation-a review. *Int. J. Curr. Microbiol. Appl. Sci* **7**, 2656-2668 (2018).

60 Song, G.-q., Prieto, H. & Orbovic, V. Agrobacterium-mediated transformation of tree fruit crops: methods, progress, and challenges. *Frontiers in plant science* **10**, 226 (2019).

61 Sugimoto, K., Gordon, S. P. & Meyerowitz, E. M. Regeneration in plants and animals: dedifferentiation, transdifferentiation, or just differentiation? *Trends in cell biology* **21**, 212-218 (2011).

62 Aida, M. *et al.* The PLETHORA genes mediate patterning of the Arabidopsis root stem cell niche. *Cell* **119**, 109-120 (2004).

63 Galinha, C. *et al.* PLETHORA proteins as dose-dependent master regulators of Arabidopsis root development. *Nature* **449**, 1053-1057 (2007).

64 Horiguchi, G., Kim, G. T. & Tsukaya, H. The transcription factor AtGRF5 and the transcription coactivator AN3 regulate cell proliferation in leaf primordia of Arabidopsis thaliana. *The Plant Journal* **43**, 68-78 (2005).

65 Liebsch, D. & Palatnik, J. F. MicroRNA miR396, GRF transcription factors and GIF co-regulators: a conserved plant growth regulatory module with potential for breeding and biotechnology. *Current opinion in plant biology* **53**, 31-42 (2020).

66 Zhang, D. *et al.* GRF-interacting factor1 regulates shoot architecture and meristem determinacy in maize. *The Plant Cell* **30**, 360-374 (2018).

67 Swinnen, G., Lizé, E., Loera Sánchez, M., Stolz, S. & Soyk, S. Application of a GRF-GIF chimera enhances plant regeneration for genome editing in tomato. *Plant biotechnology journal* **23**, 4044-4056 (2025).

68 Yasmeen, A. *et al.* In planta transformation of tomato. *Plant molecular biology reporter* **27**, 20-28 (2009).

69 Quiroz, L. F. *et al.* Tissue culture-independent approaches to revolutionizing plant transformation and gene editing. *Horticulture Research* **12**, uhae292 (2025).

70 Long, Y., Yang, Y., Pan, G. & Shen, Y. New insights into tissue culture plant-regeneration mechanisms. *Frontiers in plant science* **13**, 926752 (2022).

71 Li, X.-X. *et al.* Non-tissue culture genetic modifications for plant improvement. *Plant Molecular Biology* **115**, 67 (2025).

72 Komari, T., Hiei, Y., Saito, Y., Murai, N. & Kumashiro, T. Vectors carrying two separate T-DNAs for co-transformation of higher plants mediated by Agrobacterium tumefaciens and segregation of transformants free from selection markers. *The Plant Journal* **10**, 165-174 (1996).

73 He, Y. & Zhao, Y. Technological breakthroughs in generating transgene-free and genetically stable CRISPR-edited plants. *Abiotech* **1**, 88-96 (2020).

74 Aliaga-Franco, N. *et al.* Identification of transgene-free CRISPR-edited plants of rice, tomato, and Arabidopsis by monitoring DsRED fluorescence in dry seeds. *Frontiers in plant science* **10**, 1150 (2019).

75 Borghi, L. in *Plant Developmental Biology: Methods and Protocols* 65-75 (Springer, 2010).

76 Samalova, M., Kirchhelle, C. & Moore, I. Universal Methods for Transgene Induction Using the Dexamethasone-Inducible Transcription Activation System pOp6/LhGR in Arabidopsis and Other Plant Species. *Current Protocols in Plant Biology* **4**, e20089 (2019).

77 Sharma, P. & Lew, T. T. S. Principles of nanoparticle design for genome editing in plants. *Frontiers in Genome Editing* **4**, 846624 (2022).

78 Jiang, T. *et al.* Genome-wide analysis of the SPL gene family in lettuce and its role in miR156/SPL module mediated plant development and regeneration. *Hortic Plant J* (2025).

79 Hung, J.-H. & Weng, Z. Designing polymerase chain reaction primers using Primer3Plus. *Cold Spring Harbor Protocols* **2016**, pdb. prot093096 (2016).

80 Schwinn, K. *et al.* A small family of MYB-regulatory genes controls floral pigmentation intensity and patterning in the genus Antirrhinum. *The Plant Cell* **18**, 831-851 (2006).

81 Jyothishwaran, G. *et al.* A modified freeze–thaw method for efficient transformation of Agrobacterium tumefaciens. *Current science* **93**, 770-772 (2007).

82 Jiang, T. *et al.* Regulatory role of MicroRNA164 in heat and salinity stress responses via candidate target genes during seed germination in petunia. *Horticulture Advances* **3**, 15 (2025).

83 Hesami, M., Daneshvar, M. H., Yoosefzadeh-Najafabadi, M. & Alizadeh, M. Effect of plant growth regulators on indirect shoot organogenesis of Ficus religiosa through seedling derived petiole segments. *Journal of Genetic Engineering and Biotechnology* **16**, 175-180 (2018).

84 Mohamed, A.-a. N., Ismail, M. R. & Rahman, M. H. In vitro response from cotyledon and hypocotyls explants in tomato by inducing 6-benzylaminopurine. *African Journal of Biotechnology* **9**, 4802-4807 (2010).

85 Sharma, M. K., Solanke, A. U., Jani, D., Singh, Y. & Sharma, A. K. A simple and efficient Agrobacterium-mediated procedure for transformation of tomato. *Journal of biosciences* **34**, 423-433 (2009).

86 Rotino, G. & Gleddie, S. Transformation of eggplant (Solanum melongena L.) using a binary Agrobacterium tumefaciens vector. *Plant Cell Reports* **9**, 26-29 (1990).

87 Kiyokawa, S., Kikuchi, Y., Kamada, H. & Harada, H. Genetic transformation of Begonia tuberhybrida by Ri rol genes. *Plant cell reports* **15**, 606-609 (1996).

88 Mancini, M. *et al.* Development of a modified transformation platform for apomixis candidate genes research in Paspalum notatum (bahiagrass). *In Vitro Cellular & Developmental Biology-Plant* **50**, 412-424 (2014).

89 Karn, A. *et al.* Establishment of in vitro shoot regeneration and genetic transformation system for Southern Highbush Blueberry (SHB). *Plant Cell, Tissue and Organ Culture (PCTOC)* **163**, 1-12 (2025).

90 Zhang, Y. *et al.* A highly efficient agrobacterium-mediated method for transient gene expression and functional studies in multiple plant species. *Plant communications* **1** (2020).

91 Porebski, S., Bailey, L. G. & Baum, B. R. Modification of a CTAB DNA extraction protocol for plants containing high polysaccharide and polyphenol components. *Plant molecular biology reporter* **15**, 8-15 (1997).

92 Livak, K. J. & Schmittgen, T. D. Analysis of relative gene expression data using real-time quantitative PCR and the 2− ΔΔCT method. *methods* **25**, 402-408 (2001).

93 Wan, H. *et al.* Identification of reference genes for reverse transcription quantitative real-time PCR normalization in pepper (Capsicum annuum L.). *Biochemical and biophysical research communications* **416**, 24-30 (2011).

94 Hulse-Kemp, A. M. *et al.* Reference quality assembly of the 3.5-Gb genome of Capsicum annuum from a single linked-read library. *Horticulture research* **5** (2018).

95 Pertea, M., Kim, D., Pertea, G. M., Leek, J. T. & Salzberg, S. L. Transcript-level expression analysis of RNA-seq experiments with HISAT, StringTie and Ballgown. *Nature protocols* **11**, 1650-1667 (2016).

96 Wen, G. in *Proceedings of the 2017 international conference on biomedical engineering and bioinformatics.* 11-15.

97 Wu, T. *et al.* clusterProfiler 4.0: A universal enrichment tool for interpreting omics data. *The innovation* **2** (2021).

98 Reimann, C., Filzmoser, P., Garrett, R. & Dutter, R. *Statistical data analysis explained: applied environmental statistics with R*. (John Wiley & Sons, 2011).

99 Yazici, B. & Yolacan, S. A comparison of various tests of normality. *Journal of statistical computation and simulation* **77**, 175-183 (2007).

100 Vickers, A. J. Parametric versus non-parametric statistics in the analysis of randomized trials with non-normally distributed data. *BMC medical research methodology* **5**, 35 (2005).

101 Agbangba, C. E., Aide, E. S., Honfo, H. & Kakai, R. G. On the use of post-hoc tests in environmental and biological sciences: A critical review. *Heliyon* **10** (2024).

Acknowledgements

We are grateful to Chi Nguyen and Matthew Creech for their invaluable support in procuring chemicals, maintaining seed stocks, and managing equipment and facilities. This project was funded by the USDA-NIFA grant 2019-67013-29236, the USDA HATCH program FLA-MFC-006387, and FFAR grant A21-1857-S001, awarded to H.H.

Ethics declarations

Competing interests

The authors declare no conflict of interest.

Supplementary Information

Supplementary Fig. 1: Schematic representation of the expression vectors used for evaluating developmental regulators (DRs) in plant transformation. a, Control expression vector pOX135 containing an *eGFP-NPTII* fusion gene driven by the *CsVMV* promoter, without any DRs (NA). Single DR expression vectors are modified pOX135 constructs carrying individual DR genes (*PLT5*, *WIND1*, *IPT*, *WUS*, *GRFs*, *WOX13*, *WOX5*, *BBM*, or *ESR1*), each driven by a double *CaMV35S* promoter (2×*CaMV35S*) (see Supplementary File 2 for promoter sequence information). **b,** Double DR expression vectors are modified pOX135 constructs containing two different DR genes (*PLT5-GRFs*, *PLT5-IPT*, *PLT5-WUS*, *PLT5-WIND1*, *PLT5-ESR1*, *PLT5-WOX5*, *PLT5-WOX13*, *PLT5-BBM*, *GRFs-WOX5*, or *GRFs-WOX13*), each positioned at separate loci and driven by independent 2×*CaMV35S* promoters. **c,** Triple DR expression vectors are modified pOX135 constructs incorporating three distinct DR genes (*PLT5-GRFs-ESR1*, *PLT5-GRFs-WOX5*, *PLT5-GRFs-WOX13*, *PLT5-WUS-WOX5*, *PLT5-ESR1-WOX5*, *PLT5-ESR1-WOX13*, or *GRFs+ESR1-WOX5*), each positioned at separate loci and driven by individual 2×*CaMV35S* promoters. In all constructs, *35S-T* and *Hsp-T* represent terminators. LB and RB indicate the left and right borders of the T-DNA, respectively.

Supplementary Fig. 2: Verification of expression vector construction. a, PCR amplification of the coding sequences (CDS) of various developmental regulators (DRs) used in this study. Expected amplicon sizes (in bp) are indicated below each lane. **b,** Restriction enzyme digestion of single and double DR expression cassettes to confirm proper vector assembly. Lanes 1-7: single DR cassettes; lanes 8-14: double DR cassettes. Restriction enzymes used were EcoRI, BsaI, MluI, AatII, SpeI, SalI, and SbfI, with their recognition sites shown in the schematic representation in panel c. **c,** Schematic diagram of the restriction enzyme sites used for vector analysis. Hsp-T, heat shock protein terminator; 2×CaMV35S,

double Cauliflower Mosaic Virus 35S promoter; RB, right border. **d,** Representative gel image showing the restriction pattern of P-WUS double DR cassette digested with EcoRI, WOX5, and WOX13, confirming the correct ligation of the two DR cassettes. **e,** Restriction enzyme digestion of single and double DR expression vectors using EcoRI, WOX5, and WOX13. Expected band sizes (in bp) are indicated on the left. M, DNA size marker.

Supplementary Fig. 3: Schematic representation of expression vectors containing different visible markers and developmental regulators (DRs). a, pOX135-RUBY control vector harboring an *eGFP-NPTII* fusion gene driven by the *CsVMV* promoter and a synthetic betalain biosynthesis gene (*RUBY*) under the control of a double *CaMV35S* promoter (2×*CaMV35S*). **b,** pOX135-RUBY-PLT5-GRF4/GIF1 (PG+RU) vector, a modified pOX135-RUBY construct incorporating additional cassettes of *PLT5* (from Arabidopsis) and *GRF4*/*GIF1* (from grape), both driven by 2×*CaMV35S* promoters. **c,** pOX135-ROSEA1 control vector containing an *eGFP-NPTII* fusion gene driven by the *CsVMV* promoter and an anthocyanin regulatory gene (*ROSEA1*) under the control of 2×*CaMV35S*. **d,** pOX135-ROSEA1-PLT5-GRF4/GIF1 (PG+RO) vector, a modified pOX135-ROSEA1 construct incorporating additional cassettes of *PLT5* (from Arabidopsis) and *GRF4*/*GIF1* (from grape), both driven by 2×*CaMV35S* promoters. In all constructs, *35S-T* and *Hsp-T* represent terminators, while LB and RB indicate the left and right borders of the T-DNA, respectively.

Supplementary Fig. 4: Comprehensive screening of DRs effects on callus induction, shoot regeneration, and transformation frequency in *Petunia hybrida*. Representative images of Petunia culture plates showing leaf explant responses to various DRs on callus-induction MS medium at 2- and 3-wpi. Images were selected to represent the average response across three biological replicates, with each replicate consisting of 20 leaf explants cultured under identical conditions.

Supplementary Fig. 5: Comprehensive screening of DRs for regeneration in tomato of DR effects on callus induction, shoot regeneration, and transformation frequency in tomato (*Solanum lycopersicum* cv. Micro-Tom). a, Representative images of individual tomato explants illustrating

regeneration responses to various DR combinations at 3- (See Fig. 1a), 4-, and 5- wpi. Upper panels show individual DRs (pOX135 control, GRFs, IPT, WUS, WIND1, ESR1, WOX5, WOX13, BBM); middle panels display PLT5-based combinations (PLT5, P-GRFs, P-IPT, P-WUS, P-WIND1, P-ESR1, P-WOX5, P-WOX13, P-BBM); and lower panels present more complex combinatorial treatments (G-WOX5, G-WOX13, P-G-ESR1, P-G-WOX5, P-G-WOX13, P-W-WOX5, P-E-WOX5, P-E-WOX13, G-E-WOX5) (where P = PLT5, G = GRF4/GIF1, E = ESR1, W = WUS). **b**, Representative images of tomato culture plates showing cotyledon explant responses to various DR combinations on MS medium at 3-, 4-, and 5-wpi. Images were selected to represent the average response across three biological replicates, with each replicate consisting of 20 cotyledon explants cultured under identical conditions. Statistical analysis of the DR evaluation on tomatoes is provided in Supplementary Table 1.

Supplementary Fig. 6: Comparative analysis of developmental regulator (DR) effects on regeneration in chili pepper (*Capsicum annuum*). Representative images of individual chili pepper cotyledon explants showing regeneration responses following Agrobacterium-mediated transformation with various DR constructs at 2-, 3-, and 4- wpi. The tested constructs include pOX135 (control), PLT5, IPT, GRF4/GIF1, P-GRFs, P-IPT, P-WUS, P-WIND1, P-ESR1, P-WOX5, P-WOX13, P-BBM, and P-G-WOX13 (where P = PLT5, G = GRF4/GIF1). Images were selected from full culture plates to represent the average response across three biological replicates, with each replicate consisting of 20 cotyledon explants cultured under identical conditions. Statistical analysis of the DR evaluation on chili is provided in Supplementary Table 3.

Supplementary Fig. 7: Phenotypic characterization of *PLT5-GRFs* transgenic chili pepper (*Capsicum annuum*). a, Fluorescence microscopy of cotyledon explants and calli at 10, 28, 35, and 56 dpi with control (CK) or *PLT5-GRF4* (PG) constructs. Insets show GFP expression in transgenic PG shoots. Scale bars, 2 mm. **b,c,** Developmental comparison of T0 transgenic PG and wild-type (WT) chili pepper plants at various growth stages: seedlings at 10 weeks post-inoculation (wpi) (b, left), plants at 14 and 20 wpi (b, middle and right), flowers at 18 wpi (c, left), and seeds at 20 wpi (c, middle). GFP

fluorescence in WT and PG seeds is shown in c, right. Scale bars, 1 cm (b), 5 mm (c, left and middle), and 2 mm (c, right). **d,** Side view (top) and top view (bottom) of T1 transgenic PG and WT chili pepper plants at 10 weeks after seed germination, showing differences in plant architecture and leaf morphology. Scale bars, 5 cm. **e,** Quantification of plant height in WT and PG plants at 10 weeks after seed germination. Data are presented as mean ± s.d. (n = 6 plants per genotype, 3 biological replicates). Asterisks indicate statistically significant differences based on a two-tailed Student's t-test (***P < 0.001).

Supplementary Fig. 8: Transcriptional profiling reveals *PLT5* and *GRF*s-mediated gene expression changes associated with enhanced transformation frequencyin *Capsicum annuum*. a-c, KEGG pathway enrichment analysis of differentially expressed genes (DEGs) in *C. annuum* at 3 wpi with *PLT5-GRFs* (PG) compared to the control (CK). The analysis was performed using homologs of *C. annuum* DEGs identified in *Arabidopsis thaliana* (a), *Nicotiana tabacum* (b), and *Solanum lycopersicum* (c). Dot size represents the number of DEGs in each pathway, and color indicates the statistical significance (−log10(false discovery rate)). **d–l,** Hierarchical clustering and heatmap visualization of transcriptional profiles for genes involved in key regulatory pathways: developmental regulation (d), auxin signaling (e), cytokinin signaling (f), DNA modification (g), histone modification (k), chromatin remodeling (h), small RNA silencing (i), Polycomb Repressive Complex (PRC) interactions (j), and small RNA processing (l). Expression levels are presented as log2(transcripts per million + 1) values across three biological replicates for each treatment: CK, PLT5 alone (P), GRF4 alone (G), and PG at 1-, 2-, and 3- wpi. Color scale represents normalized expression levels from low (blue) to high (red).

Supplementary Fig. 9: Co-expression of *PLT5* and *GRF*s enhances anthocyanin accumulation and transformation frequencyin Begonia (continued in Fig. 5). a,b, Leaf explants transformed with the *ROSEA1* control plasmid (a) or the *PLT5-GRFs+ROSEA1* (PG+RO) plasmid (b) showing callus development, GFP fluorescence, and red pigmentation at 20 and 40 dpi. PG+RO explants exhibit enhanced GFP fluorescence and intense red pigmentation compared to the control. **c,d,** Phenotypic comparison of wild-type (WT) (c) and transgenic PG+RO (d) plants at 120 dpi, showing detailed views of

leaves under bright field (left) and UV illumination (right). Scale bars, 1 cm (a-d). **e,f,** Phenotypic comparison of WT (e) and PG+RO (f) plants at 150 dpi, displaying whole plant morphology (e) and anthocyanin accumulation in leaves and stems (f). PG+RO plants exhibit enhanced anthocyanin production compared to WT. Scale bars, 2 cm (e, f).

Supplementary Fig. 10: Co-expression of *PLT5* and *GRFs* enhances shoot regeneration and transformation frequencyin *Solanum aethiopicum*. a, b, Fluorescence microscopy of calli at 14- and 28- dpi with control (CK) or *PLT5-GRF4* (PG) constructs. **c, d,** Regenerated shoots at 42- dpi from CK (c) and PG (d) treatments. **e, f,** Transgenic plantlets at 90 dpi from CK (e) and PG (f) treatments. Scale bars, 5 mm. **g, h,** Transformation frequency(percentage of explants producing transgenic shoots) in CK and PG treatments at 2 weeks (g) and 3 weeks (h) post-transformation. Data are presented as mean ± s.d. (n = 4 biological replicates, each consisting of 15 explants). Asterisks indicate statistically significant differences based on a two-tailed t-test (*P < 0.05; **P < 0.01; ***P < 0.001). **i,** PCR detection of the *GFP* transgene (450 bp) in T0 transgenic seedlings from CK and PG treatments. Wild-type (WT) plants served as a negative control.

Supplementary Fig. 11: PLT5 and GRF co-expression enhances regeneration and transformation frequency in lettuce (*Lactuca sativa*). a,c,e, Developmental progression of cotyledon explants transformed with the control vector pOX135-RUBY (RU) from 21 to 120 days post-inoculation (dpi). RU explants developed calli with weak GFP fluorescence and red pigmentation. Representative shoots at 28 dpi (c, white arrowhead) show limited GFP fluorescence. Shoot at 35 dpi (e) and fully regenerated RU plants at 90 and 120 dpi exhibited normal green phenotypes without noticeable detectable pigment accumulation in vegetative or reproductive tissues. The representative culture plate at 35 dpi (c, top right) demonstrates the limited shoot regeneration and transformation frequency of the RU construct. **b,d,f,** Developmental progression of cotyledon explants transformed with the *PLT5-GRFs+RUBY* (PG+RU) vector from 21 to 120 dpi. PG+RU explants showed strong GFP fluorescence and red pigmentation. Representative shoots at 28 dpi (d, red arrowhead) and displays strong GFP fluorescence. Fully

regenerated PG+RU plants at 90 and 120 dpi exhibited strong red pigmentation in leaves, stems, and flowers. The representative culture plate at 35 dpi (d, bottom right) demonstrates the enhanced shoot regeneration and transformation frequency of the PG+RU construct. Red arrowheads denote the regenerated shoots from PG+RU, while white arrowheads indicate those from RU. Scale bars, 2 mm (a,b), 1 mm (c,d), 1 cm (e,f). **g,** Regeneration frequency (percentage of explants producing shoots) and transformation frequency(percentage of explants producing transgenic shoots) in RU and PG+RU treatments at 4 wpi. Data are presented as mean ± s.d. (n = 3 biological replicates, each consisting of 15 explants). Asterisks indicate statistically significant differences based on a two-tailed Student's t-test (**P < 0.01).

Supplementary Fig. 12: Co-expression of PLT5 and GRFs enhances genetic transformation frequency in blueberry using the *ROSEA1* visible marker. a–**c** Representative shoot-regenerating explants of *Vaccinium corymbosum* 'Albus' transformed with pOX135 empty vector (CK) (**a**), pOX135-*ROSEA1* (ROSEA) (**b**) and pOX135-PG+RO (PLT5+GRFs+*ROSEA1*) (**c**) at 49 days post inoculation (dpi), shown under bright field (left) and fluorescence (right). **d**, **e** Additional pOX135-PG+RO explants at later time points (49 and 56 dpi, as indicated), highlighting pink anthocyanin pigmentation and GFP fluorescence in emerging shoots. **f**–**h** Whole regeneration plates at 63 dpi for CK (**f**), ROSEA (**g**) and PG+RO (**h**). **i**, **k** PCR detection of the *AmROSEA1* transgene (450 bp) in independent transformants. **j**, **m** PCR detection of the *eGFP* transgene (630 bp) in the same samples. For each gel, lane 1, 1 kb Plus DNA ladder; lane 2, plasmid positive control (pOX135-*ROSEA1* in **i**–**j**; pOX135-PG+RO in **k**–**m**); lane 3, water negative control; lane 4, wild-type 'Albus'; lanes 5–9 (**i**–**j**) or 5–11 (**k**–**m**), independent putative transformants. **n** Transformation frequency of each construct calculated as the percentage of PCR-positive shoots among total regenerated shoots. Scale bars, as indicated.

Supplementary Table 1: Effects of developmental regulators (DRs) on plant regeneration and transformation in *Petunia hybrida*.

Supplementary Table 2: Effects of DRs on plant regeneration and transformation in tomato (*Solanum lycopersicum* cv. Micro-Tom).

Supplementary Table 3: Effects of developmental regulators (DRs) on plant regeneration and transformation in chili pepper (*Capsicum annuum*).

Supplementary Table 4: Primers for vector construction, genotyping, and gene expression analysis.

Figures

Fig. 1: Evaluation of developmental regulator (DR) combinations on transformation efficiency.

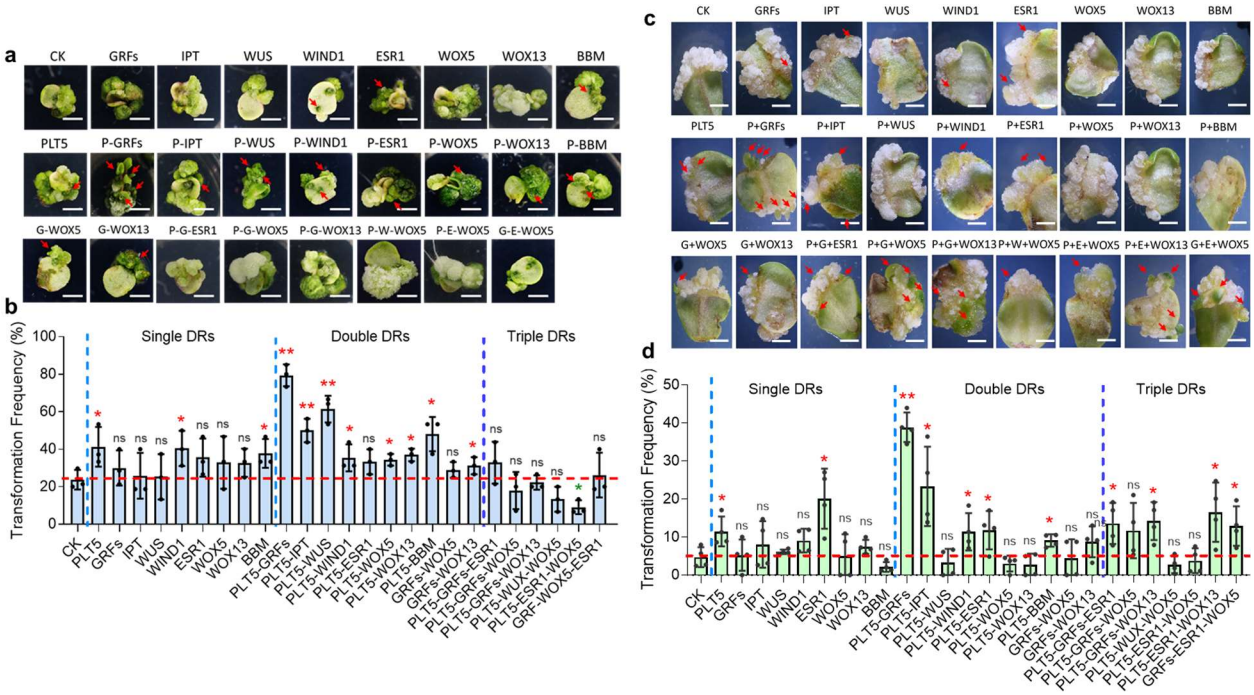

a, c Representative images of regenerated explants at 3 weeks post-inoculation (wpi) in petunia and 4 wpi in tomato with the indicated DR constructs (See Supplementary Fig. 1 for details on constructs). Red arrowheads highlight shoot primordia formation. The tested DRs include pOX135 (control, labeled with CK), *GRF4/GIF1*, (labeled with *GRFs*), *IPT*, *WUS*, *WIND1*, *ESR1*, *WOX5*, *WOX13*, *BBM*, *PLT5*, *P-GRFs*, P-IPT, P-WUS, P-WIND1, P-ESR1, P-WOX5, P-WOX13, P-BBM, P-G-ESR1, P-G-WOX5, P-G-WOX13, P-W-WOX5, P-E-WOX5, P-E-WOX13, G-WOX5, G-WOX13, and G-E-WOX5 (where P = PLT5, G = GRF4/GIF1, E = ESR1, W = WUS). **b, d** Transformation frequency (percentage of explants producing transgenic shoots) in response to different DR combinations at 3 wpi in petunia and 4 wpi in tomato, respectively. Data are presented as mean ± s.d. (n = 4, 20 explants each, ns, not significant; $*P < 0.05$; $**P < 0.01$). Explants were derived from cotyledons of the tomato variety "Micro-Tom." See also Supplementary Fig.5 and Supplementary Table 2.

Fig. 2: Enhanced transformation of chili pepper (*Capsicum annuum*) using *PLT5-GRFs*.

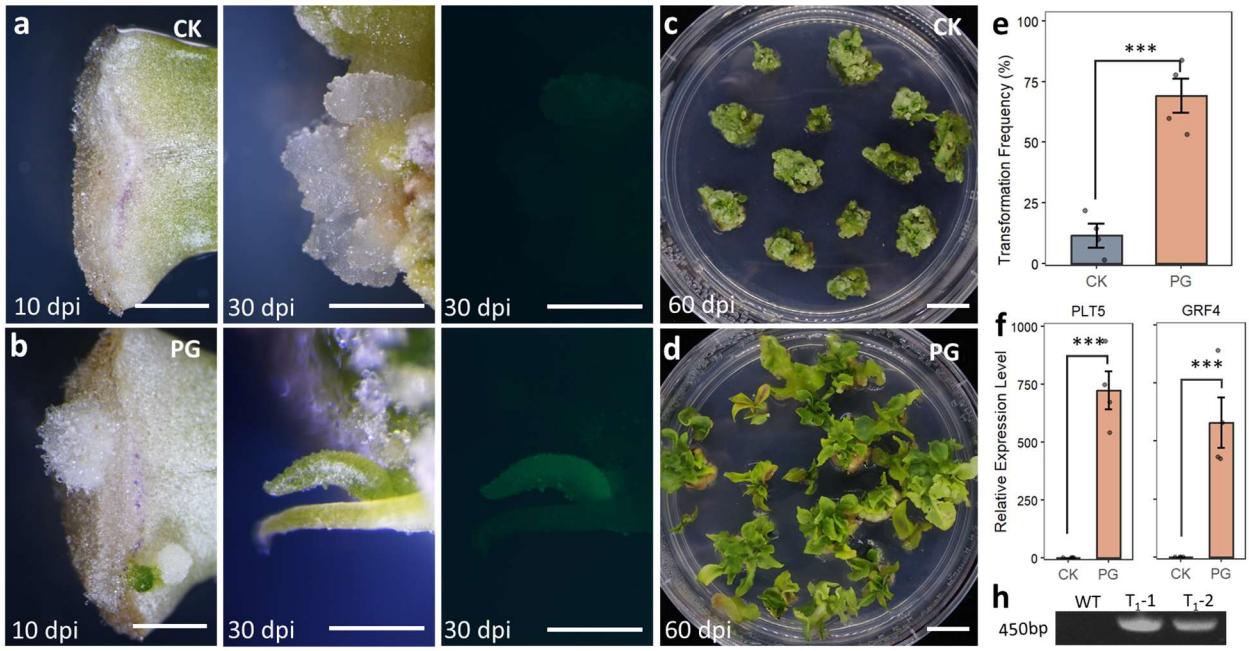

a, b, Fluorescence microscopy of cotyledon explants and calli at 10- and 30 days post-infection (dpi) with control (CK) or *PLT5-GRFs* (PG) constructs. Regenerated shoots at 30 dpi show GFP expression in transgenic PG shoots. **c, d,** Regenerated shoots at 60 dpi from CK (c) and PG (d) treatments. **e,** Transformation frequency (percentage of explants producing transgenic shoots) in CK and PG treatments. Data are presented as mean ± s.d. (n = 4, 15 explants each, ***P < 0.001.). **f,** Relative expression of *PLT5* and *GRF4* in CK and PG explants at 3 wpi, normalized to the reference gene *CaGAPDH* (n = 3, **P < 0.001). **h,** Molecular confirmation of transgene presence: PCR detection of GFP (450 bp) in T_1 transgenic seedlings (PG), with wild type (WT) as the negative control. Scale bars, 1 cm. See also Supplementary Fig. 6 and 7.

Fig. 3: Transcriptomic analysis reveals *PLT5* and *GRF*-mediated regulation of plant regeneration genes in chili pepper (*Capsicum annuum*).

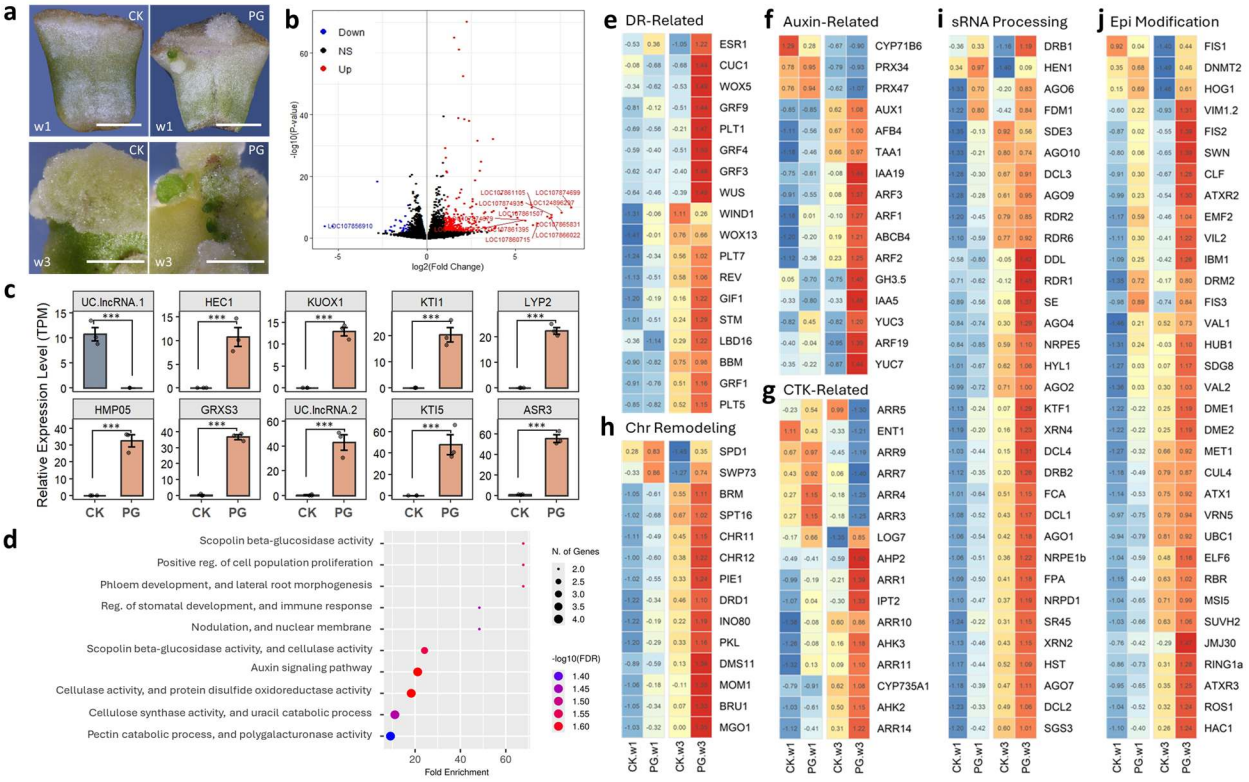

a, Calli and shoots from explants transformed with control (CK) or *PLT5-GRFs* (PG) at 1- and 3 wpi. Scale bars, 5 mm. **b,** Volcano plot of DEGs at 1 and 3 wpi. Red and blue dots indicate significantly up- and down-regulated genes, respectively. **c,** Top 10 DEGs (mean ± s.d., n = 3, ***P < 0.001). **d,** KEGG enrichment of DEGs. Dot size represents the number of DEGs per pathway, and color indicates the statistical significance (−log10(false discovery rate)). **e–j,** Heatmaps of DEGs for developmental regulators (DRs) (e), auxin (f) and cytokinin (g) pathways, chromatin remodeling (h), small RNA processing (i), and epigenetic regulation (j) at 1- and 3 dpi. See also Supplementary Fig. 8.

Fig. 4: *PLT5-GRFs* promote shoot regeneration and enhance transformation efficiency in Begonia.

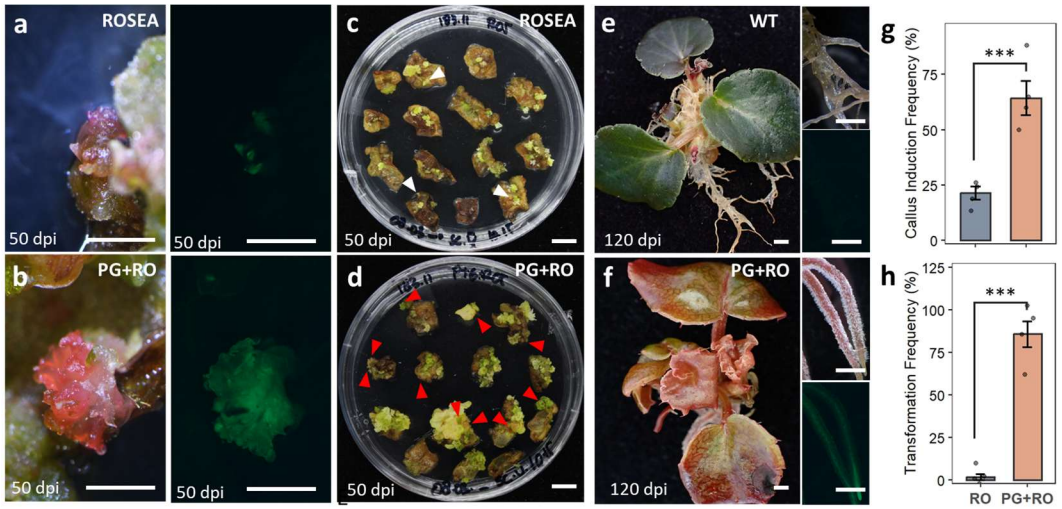

a,b, Callus with weak (a) or intense (b) GFP and anthocyanin accumulation at 50 dpi with *ROSEA* control and *PLT5-GRFs-ROSEA1* (PG+RO), respectively. **c,d,** Plates at 50 dpi showing shoots (arrows) from *ROSEA* (c) or PG+RO (d). White and red arrowheads highlight reddish shoot primordia in *ROSEA* and PG+RO, respectively. **e,f,** Phenotypic comparison of wild-type (WT) (e) and transgenic PG+RO (f) plants at 120 dpi, showing whole plant morphology and detailed views of roots under bright field (top) and UV illumination (bottom). **g,h,** Callus Induction (g) and transformation (h) frequency (mean ± s.d., n = 4, 15 explants each). ***P < 0.001 (Student's t-test). Scale bars, 1 cm. See also Supplementary Fig. 9.

Fig. 5: *PLT5* and *GRFs* co-expression enhances genetic transformation efficiency in blueberry (*Vaccinium corymbosum*) using the ROSEA1 anthocyanin marker.

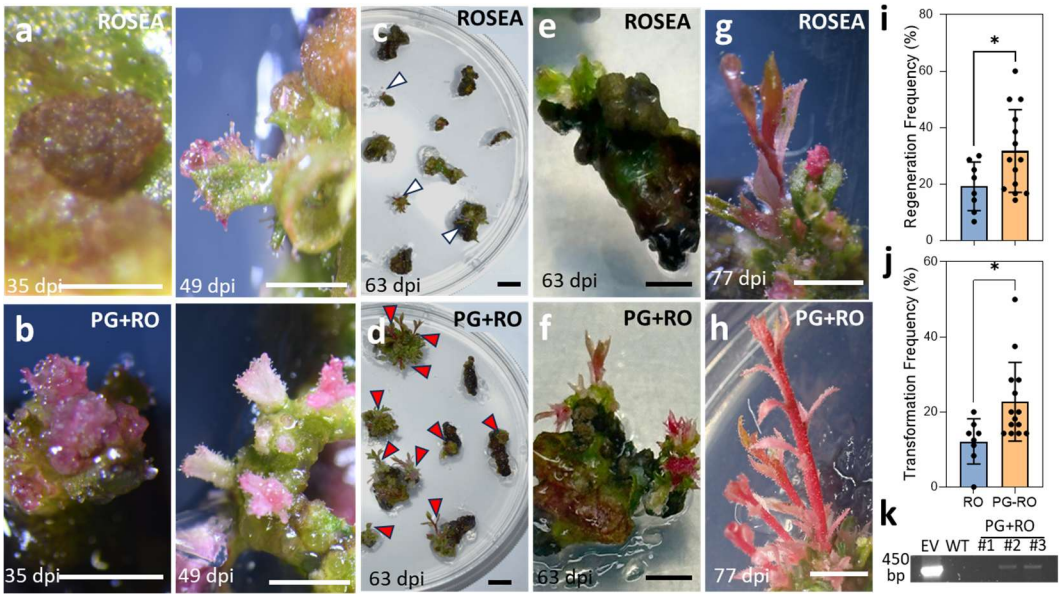

a,c,e,g, Developmental progression of young leaf explants transformed with the control vector pOX135-ROSEA1 (RO) from 28 to 70 days post-inoculation (dpi). RO explants developed calli with weak or no GFP fluorescence and red pigmentation. Representative shoots at 28 and 35 dpi (a, white arrowheads) show no GFP fluorescence. Regenerated shoots at 56 (c,e) and 70 dpi (g) exhibited normal green phenotypes without detectable pigment accumulation in vegetative tissues. The representative culture plate at 56 dpi (c,e) demonstrates smaller calli and limited shoot regeneration and transformation frequency of the RO construct. **b,d,f,h,** Developmental progression of young leaf explants transformed with the *PLT5-GRFs-ROSEA1* (PG+RO) vector from 28 to 70 dpi. PG+RO explants showed strong GFP fluorescence and red pigmentation. Representative shoots at 28 and 35 dpi (b, red arrowheads) display strong GFP fluorescence. Regenerated PG+RO shoots at 56 and 70 dpi exhibited strong pinkish pigmentation in leaves and stems. The representative culture plate at 56 dpi (d,f) demonstrates the enhanced shoot regeneration and transformation frequency of the PG+RO construct. Red arrowheads denote the regenerated shoots with typical pinkish pigmentation from PG+RO, while white arrowheads indicate those from RO. Scale bars, 2 mm (a,b), 5 mm (c,d), 1 cm (e,f), 2 cm (g,h). **i,j,** Regeneration frequency (i) and transformation frequency (j) in RO and PG+RO treatments at 9 wpi. Data are presented as mean ± s.d. (n = 10 biological replicates, each consisting of 10 explants). Asterisks indicate statistically significant differences based on a two-tailed Student's t-test (ns, not significant; **P < 0.01). **k,** PCR detection of the *GFP* transgene (450 bp) in T0-1 and T0-2 transgenic plants from the PG+RO treatment. Wild-type (WT) plants served as a negative control.

Fig. 6: *PLT5* and *GRF*s co-expression enhances genetic transformation efficiency in bahiagrass (*Paspalum notatum*).

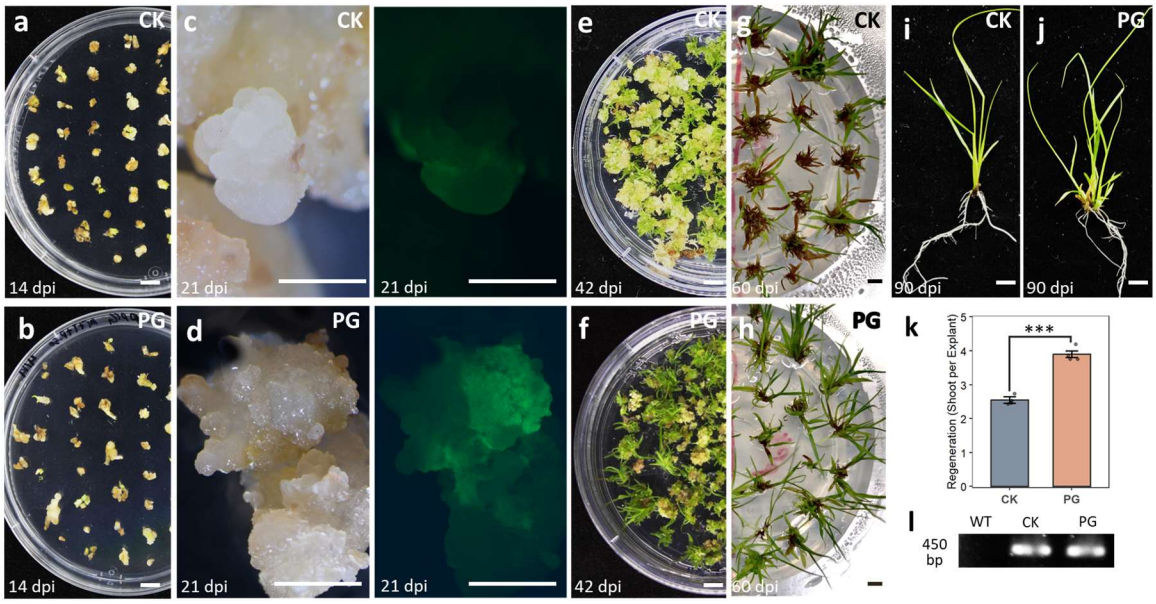

a,b, Fluorescence microscopy of calli derived from leaf explants at 14 dpi with control (CK) or *PLT5-GRFs* (PG) constructs. **c,d,** CK calli (c) exhibit weak GFP fluorescence, while PG calli (d) show strong GFP signal at 21 dpi. **e,f,** Representative culture plates demonstrating shoot regeneration at 42 dpi from CK (e) and PG (f) treatments. PG shoots display enhanced growth and development compared to CK. The PG plate shows a significantly higher number of regenerated shoots than CK. **g,h,** Transgenic plantlets at 60 dpi from CK (g) and PG (h) treatments. PG plantlets exhibit more vigorous growth and increased biomass. **i,j,** Transgenic plants derived from CK (i) and PG (j) treatments, revealing striking differences in tiller number and overall plant architecture. **k,** Quantification of transformation frequency, expressed as the number of regenerated shoots per explant, in CK and PG treatments. Data are presented as mean ± s.d. (n = 4, 15 explants each, ***P < 0.001). **l,** PCR detection of the *GFP* transgene (450 bp) in T0 transgenic plants from the CK and PG treatments. Wild-type (WT) plants served as a negative control. Scale bars, 1.5 cm.

Fig. 7: *PLT5-GRFs* enhances *in-planta* transformation efficiency in *Sinningia speciosa*.

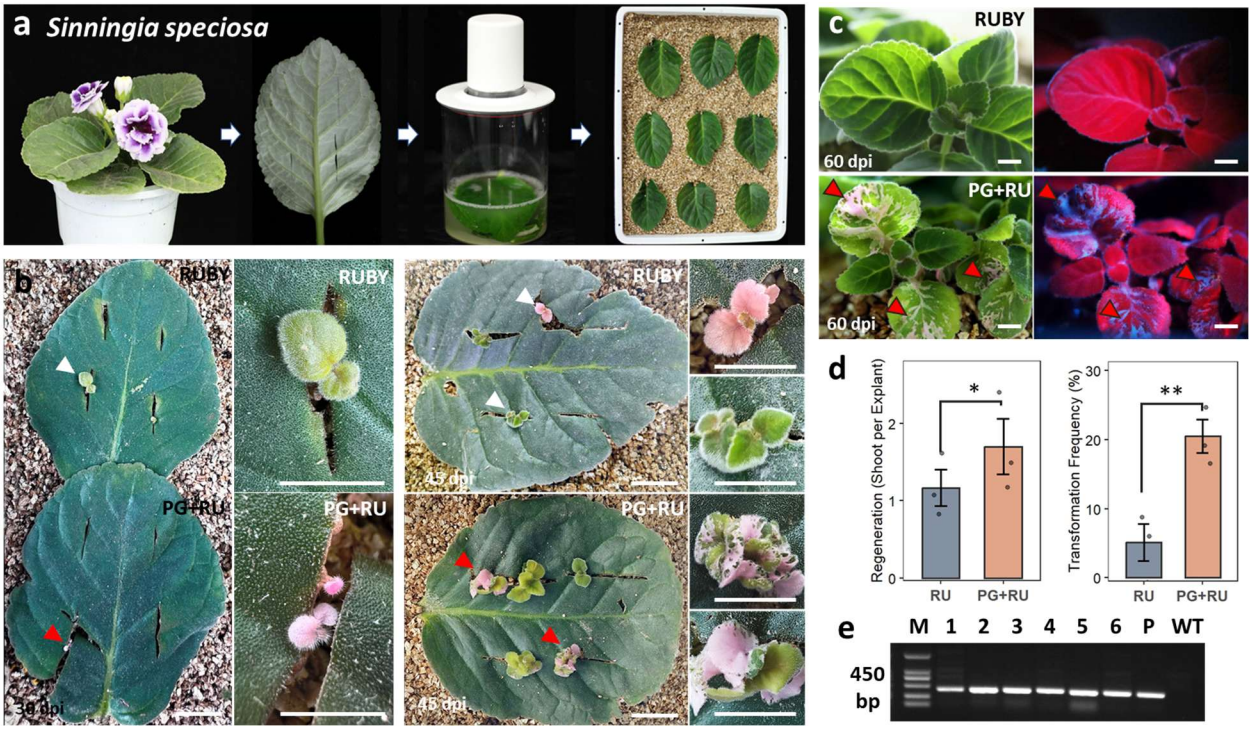

a, Schematic of the *in-planta* transformation protocol: mature leaves from healthy 4-5-month-old plants were scratched before being immersed in *Agrobacterium* suspension. A vacuum infiltration step was applied, followed by incubation under low-light conditions. Leaves were then transferred to indoor culture, with petioles buried in vermiculite for further growth. **b,** Emergence of calli and shoots at wound sites in leaves transformed with *RUBY* (RU) or *PLT5-GRFs-RUBY* (PG+RU) constructs at 30-, 45-, and 60 dpi. Betalain accumulation and GFP fluorescence indicate successful transformation. Red arrowheads denote the regenerated shoots from PG+RU, while white arrowheads denote those from RU. **c,** GFP fluorescence in PG+RU and RU transformants at 60 dpi. Red triangles denote the betalain pigmentation and GFP signal. **d,** Regeneration frequency (percentage of explants producing shoots) and transformation frequency (percentage of explants producing transgenic shoots) in RU and PG+RU treatments. Data are presented as mean ± s.d. (n = 3, 10 explants each, *P < 0.05; **P < 0.01). **e,** PCR detection of the *GFP* transgene (450 bp) in T0 transgenic seedlings (lanes 1–6) from the PG+RU. WT plants served as a negative control, and PG+RU plasmid (P) served as a positive control. Scale bars, 1 cm.

Fig. 8: *PLT5* and *GRF/GIF1* synergistically enhance de novo shoot regeneration by coordinating developmental, hormonal, and epigenetic networks.

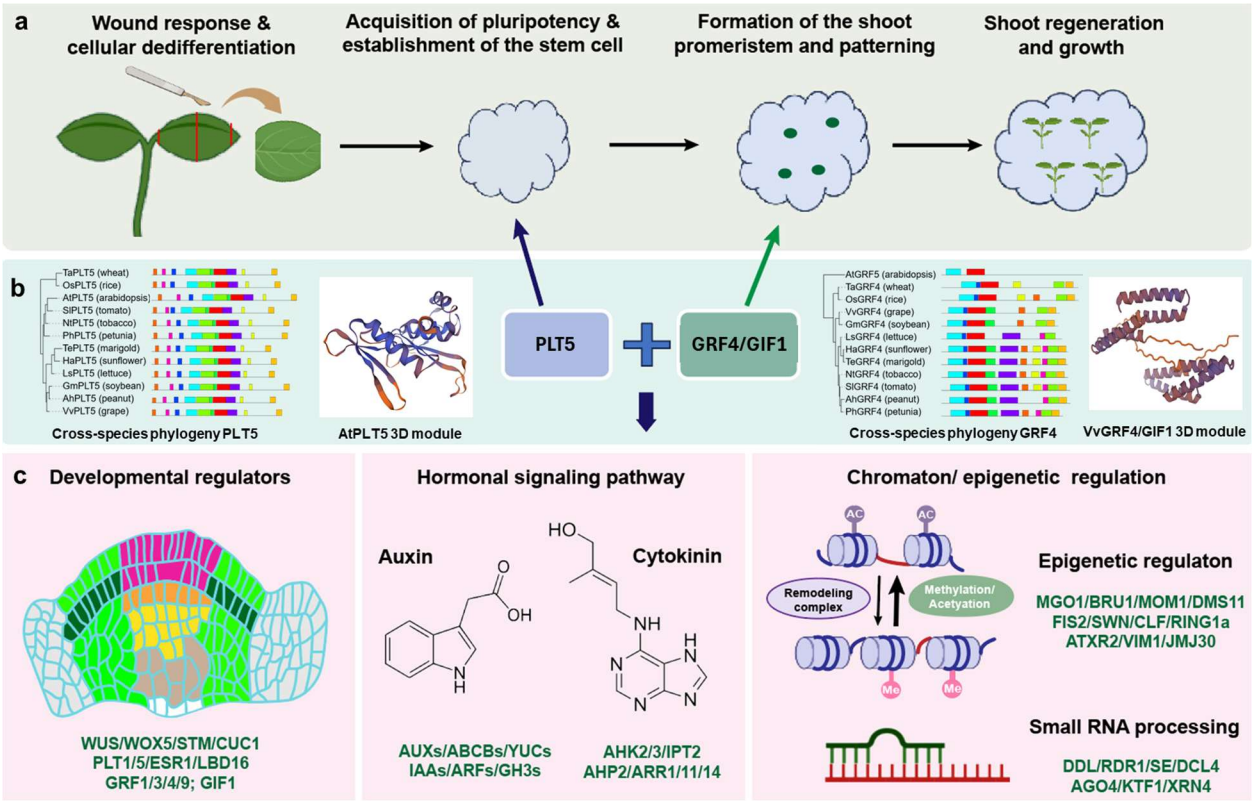

a depicts a simplified progression from wounded leaf explants to regenerated shoots. *PLT5* (blue) promotes early steps, including wound-induced dedifferentiation, callus formation and acquisition of pluripotency, and helps establish a stem-cell–like niche competent for shoot fate. *GRF4/GIF1* (green) mainly reinforces later stages by stimulating cell proliferation, shoot promeristem formation/patterning, and subsequent shoot growth. **b** cross-species phylogenetic trees of PLT5 (left) and GRF4 (right) orthologs from representative monocot and dicot species, with corresponding protein motif architectures shown as colored blocks. Predicted 3D structures of AtPLT5 and VvGRF4/GIF1 modules are displayed in the center. Species include wheat, rice, Arabidopsis, tomato, tobacco, petunia, sunflower, lettuce, soybean, peanut, and grape. **c** summarize downstream regulatory layers influenced by this module. Developmental regulators include meristem organizers and regeneration factors (for example, WUS, WOX5, STM, CUC1, PLT1/5, ESR1, LBD16, GRF1/3/4/9, and *GIF1*). Hormonal signaling pathways encompass auxin and cytokinin biosynthesis, transport, and signaling components (for example, AUX/YUC/ABCB, IAA/ARF/GH3, AHK2/3/IPT2, AHP2, and *ARR1/10/11/14*). Chromatin/epigenetic regulation (*MGO1*, *BRU1*, *MOM1*, *DMS11*, *FIS2*, *SWN*, *CLF*, *RING1a*, *ATXR2*, *VIM1* and *JMJ30*) and small RNA processing (*DDL*, *RDR1*, *SE*, *DCL4*, *AGO4*, *KTF1* and *XRN4*) further modulate regeneration competence and outcome.

Supplementary Files

This is a list of supplementary files associated with this preprint. Click to download.

- SupplementaryInformation.pdf